



U.S. DEPARTMENT OF  
**ENERGY**

PNNL-20840

Prepared for the U.S. Department of Energy  
under Contract DE-AC05-76RL01830

# Low-Intrusion Techniques and Sensitive Information Management for Warhead Counting and Verification: FY2011 Annual Report

KD Jarman  
SM Robinson  
BS McDonald  
AJ Gilbert  
AC Misner

WK Pitts  
TA White  
A Seifert  
EA Miller

September 2011



**Pacific Northwest**  
NATIONAL LABORATORY

*Proudly Operated by **Battelle** Since 1965*

## DISCLAIMER

This report was prepared as an account of work sponsored by an agency of the United States Government. Neither the United States Government nor any agency thereof, nor Battelle Memorial Institute, nor any of their employees, makes **any warranty, express or implied, or assumes any legal liability or responsibility for the accuracy, completeness, or usefulness of any information, apparatus, product, or process disclosed, or represents that its use would not infringe privately owned rights.** Reference herein to any specific commercial product, process, or service by trade name, trademark, manufacturer, or otherwise does not necessarily constitute or imply its endorsement, recommendation, or favoring by the United States Government or any agency thereof, or Battelle Memorial Institute. The views and opinions of authors expressed herein do not necessarily state or reflect those of the United States Government or any agency thereof.

PACIFIC NORTHWEST NATIONAL LABORATORY

*operated by*

BATTELLE

*for the*

UNITED STATES DEPARTMENT OF ENERGY

*under Contract DE-AC05-76RL01830*

Printed in the United States of America

Available to DOE and DOE contractors from the  
Office of Scientific and Technical Information,  
P.O. Box 62, Oak Ridge, TN 37831-0062;  
ph: (865) 576-8401  
fax: (865) 576-5728  
email: reports@adonis.osti.gov

Available to the public from the National Technical Information Service,  
U.S. Department of Commerce, 5285 Port Royal Rd., Springfield, VA 22161  
ph: (800) 553-6847  
fax: (703) 605-6900  
email: orders@ntis.fedworld.gov  
online ordering: <http://www.ntis.gov/ordering.htm>



This document was printed on recycled paper.

(9/2003)

# **Low-Intrusion Techniques and Sensitive Information Management for Warhead Counting and Verification: FY2011 Annual Report**

KD Jarman	WK Pitts
SM Robinson	TA White
BS McDonald	A Seifert
AJ Gilbert	EA Miller
AC Misner	

September 2011

Prepared for the Department of Energy Office of Non-Proliferation and Verification Research and Development (NA-22) under U.S. Department of Energy Contract DE-AC05-76RL01830

Pacific Northwest National Laboratory  
Richland, Washington 99352

\* Corresponding author: [kj@pnnl.gov](mailto:kj@pnnl.gov)

## Executive Summary

Future arms control treaties may push nuclear weapons limits to unprecedented low levels and may entail precise counting of warheads as well as distinguishing between strategic and tactical nuclear weapons. Such advances will require assessment of form and function to confidently verify the presence or absence of nuclear warheads and/or their components. Imaging with penetrating radiation can provide such an assessment and could thus play a unique role in inspection scenarios. Yet many imaging capabilities have been viewed as too intrusive from the perspective of revealing weapon design details, and the potential for the release of sensitive information poses challenges in verification settings. A widely held perception is that verification through radiography requires images of sufficient quality that an expert (e.g., a trained inspector or an image-matching algorithm) can verify the presence or absence of components of a device. The concept of information barriers (IBs) has been established to prevent access to relevant weapon-design information by inspectors (or algorithms), and has, to date, limited the usefulness of radiographic inspection. The challenge of this project is to demonstrate that radiographic information can be used behind an IB to improve the capabilities of treaty-verification weapons-inspection systems.

Pacific Northwest National Laboratory (PNNL) is supported by the Department of Energy Office of Nonproliferation and Verification Research and Development to develop image analysis and feature extraction techniques for robust component identification that eliminate the need to store sensitive reference images or sensitive image parameters. Focusing primarily on radiographic imaging, these techniques include identification of features that discriminate between different materials, reduction of images to non-sensitive summary data to allow the storage and comparison of references, and further measures of consistency using correlations between active and passive images. A main objective is to build on previously developed techniques to establish robustness to variations in radiation material and shielding configurations and for a variety of imaging technologies.

Project goals are

- Year 1 – Refine and extend previous PNNL techniques for verifying stored fissile material, focusing on nuclear weapons and weapon component verification and counting.
- Year 2 – Apply techniques and analysis to images from real imaging systems and define general system requirements for use of the techniques. Integrate techniques with prototype IB concepts.
- Year 3 – Analyze performance for warhead verification and counting.

This report summarizes our progress in Year 1.

### **Year 1 Accomplishments**

The bulk of our work during this first year was reported in three papers presented at the Institute of Nuclear Materials Management Annual Meeting in July, 2011. The basis for this effort, founded in previous algorithm development, was compiled in an article in *Nuclear Instruments and Methods, A*. These four papers are attached as appendices. A summary of our accomplishments is given below.

We began by defining specific verification problems of interest and surveying imaging capabilities. Directed by NA-22 to consider both nuclear weapon dismantlement and warhead verification and counting scenarios, we defined a phased approach in terms of three object-of-interest scenarios: the AT-400R storage container used at the Mayak Fissile Material Storage Facility and two nominal nuclear weapons. These objects represent a range of complexity in content and configuration, from dismantled

components to multiple warheads on a missile, for which adequate simulated images may be produced using Pacific Northwest National Laboratory resources.

A survey of imaging technologies, primarily focused on radiography (emission, transmission, and induced emission), was undertaken to complete this “scenarios” picture. The technologies reviewed included fast-neutron scatter cameras, coded aperture (gamma and neutron), Compton cameras and hybrid coded aperture-Compton systems; X-ray, gamma-ray, and neutron radiography; and multi-modality systems such as combined fast neutron and gamma-ray radiography (FNCR), gamma-ray combined with LIDAR, and combined emission/transmission computed tomography. While emphasizing application to a range of imaging systems, we initiated contacts with individuals developing specific systems for potential algorithm benchmarking; focusing our attention on capabilities at Oak Ridge National Laboratory (ORNL), including fast neutron coded aperture systems and tomographic imaging systems such as the Nuclear Materials Identification System and Advanced Portable Neutron Imaging System. It is our intent to combine our techniques with promising imaging technology. In particular, applying our algorithms to multi-modal systems such as those developed at ORNL may prove especially fruitful.

Our image analysis techniques follow two primary paths. The first path broadly considers extracting physical features from radiographic images, such as material composition and attenuation characteristics. These features have been estimated in PNNL’s past work by employing assumptions regarding 3D geometric distribution of material, allowing for a limited evaluation of overall density and attenuation characteristics. Results were extended by considering the energy profile of attenuated photons measured by an X-ray radiography system and photon-counting detectors. Both spectral methods for contrast improvement and spectral and dual-energy methods for material discrimination may enhance previous attempts to discern materials within transmission and emission radiography images. These methods may increase the contrast between SNM and shielding materials, improving determination of the presence of nuclear materials, allowing for a simple yes/no metric for SNM detection to be developed. With further study, these methods may prove useful for the verification of objects in both warhead counting and dismantlement verification settings.

The second image-analysis path relies on generating image transformations that can be used in templating to verify the presence or absence of weapons or weapons components. The key to such transformations is that they must be “non-invertible”—destroying the ability to reconstruct details of the original image—yet rich enough in information to enable a confident presence/absence decision. Greater reduction of image information provides greater assurance against possible release of sensitive information, but enough reduction can destroy the ability to verify. The concept of “perceptual hash” was shown to be able to incorporate and enhance the histogram approach developed earlier. Using perceptual hashing as a framework for transformations with provable non-invertibility and confident verification, we studied the degree of information reduction that maintains verification on a set of test object images using histograms, and considered how image details might be reconstructed from the histogram. The appeal of the perceptual hash concept lies in its reliance on well-established cryptographic hash results and the acceptance of hashing in IB technology. Perceptual hashing may allow templates to be used without the need to store sensitive data, and has broad potential application for enabling imaging in arms control.

### **Next Steps**

In the following two years of the project, we plan to finalize further refinements to the techniques, demonstrate the integration of the techniques with formal IB principles, test the techniques on images taken in laboratory and campaign settings (as available), and analyze their performance. Specific items to be addressed include:

- Integrating spatial constraints, based on estimates of three-dimensional structure, to improve the current pixel-by-pixel material discrimination/recognition techniques;
- Determining requirements for realistic imaging systems to enable the use of these techniques;
- Testing histograms for verification using known objects and “spoof” objects for a variety of characteristic images;
- Designing and implementing an approach to “attack” histograms to reveal details of the original images;
- Extending the techniques to apply to neutron interrogation-based systems and potentially other imaging systems;
- Combining the algorithms with imaging technology developed to benchmark results with measured data and further determining imaging system requirements in terms of algorithm performance.

## **Acknowledgments**

This research was sponsored by the U.S. Department of Energy National Nuclear Security Administration Office of Nonproliferation and Verification Research and Development (NA-22). Pacific Northwest National Laboratory is operated for the U.S. Department of Energy by Battelle under contract DE-AC05-76RL01830.

## Acronyms and Abbreviations

FY	fiscal year
IB	information barrier
INMM	Institute of Nuclear Materials Management
ORNL	Oak Ridge National Laboratory
PNNL	Pacific Northwest National Laboratory
RV	Re-entry Vehicles
SNM	special nuclear material

# Contents

1	Introduction .....	1
1.1	Summary of FY2011 Research .....	1
2	Verification Scenarios .....	3
2.1	Verification Objects .....	3
2.2	Survey of Imaging Technology.....	3
2.3	Simulations, Benchmark Images, and Test Images .....	5
3	Verification Algorithms .....	6
3.1	Material Discrimination for Attributes .....	6
3.2	Non-invertible Transforms for Templates .....	11
4	Conclusions .....	15
	References.....	17
	Appendix A: Image-based Verification: Some Advantages, Challenges, and Algorithm-driven Requirements (PNNL-SA-80551).....	18
	Appendix B: Image-Based Verification Algorithms for Arms Control (PNNL-SA-80768).....	29
	Appendix C: Non-Invertible Transforms for Image-Based Verification (PNNL-SA-80555) .....	40
	Appendix D: Imaging for Dismantlement Verification: Information Management and Analysis Algorithms [NIM-A] article; (PNNL-SA-78495).....	50

## Figures

Figure 2.1. A1: Dimensions, Weights, Centers of Gravity, Case Features, A2: View through Access Doors, Geiger Counter, A3: Neutron Counter and Gamma-spectrometer, A4: X-ray Plate Examination, A5: (untested) Full Access to Weapon Disassembly. The ideal method would be in the top-left corner with 100% discrimination and zero intrusiveness. .... 4

Figure 3.1. Energy-dependent Passive Image Object Separation ..... 8

Figure 3.2. Mass Attenuation Coefficients of Four Materials Used in the AT-400R Storage Container. Total cross-sections were obtained from the ENDF cross section libraries from the National Nuclear Data Center..... 10

Figure 3.3. Histogram Coarsening Defined by Number of Intensity Bins and Quantization of Frequency Levels ..... 12

Figure 3.4. Histogram Comparison: Effect of Coarsening on Verification with the Marinelli Beaker Test Case ..... 13

Figure 3.5. Notional Histogram-based Verification Curve ..... 14

Figure 4.1. Creating a Non-sensitive Reduction of the Image ..... 15

# 1 Introduction

Future arms control treaties may push nuclear weapons limits to unprecedented low levels and may entail precise counting of warheads as well as distinguishing between strategic and tactical nuclear weapons. Such advances will require assessment of form and function to confidently verify the presence or absence of nuclear warheads and/or their components. Imaging with penetrating radiation can provide such an assessment and could thus play a unique role in inspection scenarios. Yet many imaging capabilities have been viewed as too intrusive from the perspective of revealing configuration details of devices, and the potential for the release of sensitive information poses challenges in verification settings. In particular, using a reference image for comparison requires storing sensitive information in non-volatile memory, which increases Information Barrier (IB) design complexity (The Joint United States DOE-DOD Information Barrier Working Group, 1999). A widely held perception is that verification through radiography requires images of sufficient quality that an expert (e.g., a trained inspector or an image-matching algorithm) can verify the presence or absence of components of a device. The principle of information barriers (IBs) has been established to prevent access to relevant weapon-design information by inspectors (or algorithms), and has, to date, limited the usefulness of radiographic inspection. The challenge of this project is to demonstrate that radiographic information can be used behind an IB to improve the capabilities of treaty-verification weapons-inspection systems.

Pacific Northwest National Laboratory (PNNL) is supported by the Department of Energy Office of Nonproliferation and Verification Research and Development to develop image analysis and feature extraction techniques for robust component identification that eliminate the need to store sensitive reference images or sensitive image parameters. This work builds on a multiyear LDRD project in which PNNL explored passive and active radiography image analysis for weapons dismantlement (Pitts et al. 2010, Robinson et al. 2010) (see full paper in Appendix D). These methods included development and use of radiography with high energy X-ray sources, autoradiography with radiation imaging detectors, and an initial study of information barrier requirements. The image analysis methods included simple (non-sensitive) identification of features that discriminate between different materials, reduction of imaging data to histogram-based summaries for comparison to non-sensitive references, and further measures of consistency using correlation between active and passive images. In the LDRD effort, the methods relied on several simplifying assumptions, such as the separation of objects in the images, known geometry of imaged objects, and limited image noise. Additionally, the robustness and security (in terms of the inability to extract sensitive information) of histogram-based methods was not yet well established. The first objective of this project is to further develop the techniques, establishing robustness by studying their sensitivity to variations in radiation material, shielding configurations, and to a variety of imaging technologies, and studying the non-invertibility of image histogram-based templates. Subsequent objectives are to demonstrate the integration of methods with IB principles for use with specific systems, test the techniques in laboratory and campaign settings, and analyze their performance.

## 1.1 Summary of FY2011 Research

To carry out this effort, the specific verification problems of interest and imaging capabilities needed to be defined. Directed by NA-22 to consider both dismantlement and warhead verification and warhead counting scenarios, our first task was to define the scenarios in terms of a set of objects of interest that represent a range of content and configuration from dismantled components to multiple warheads on a missile. A survey of imaging technologies, primarily focused on radiography (emission, transmission,

and induced emission), was undertaken to complete this “scenarios” picture. While emphasizing application to a range of imaging systems, we initiated contacts with individuals developing specific systems for potential benchmarking of algorithms, focusing our attention on capabilities at Oak Ridge National Laboratory (ORNL) including fast neutron coded aperture systems and tomographic imaging systems such as the Nuclear Materials Identification System and Advanced Portable Neutron Imaging System. It is our intent to combine our techniques with promising imaging technology at ORNL.

Our image analysis techniques follow two primary paths. The first path broadly considers extracting physical features from radiographic images, such as material composition and attenuation characteristics. Extraction of quantitative information from any radiography image suffers from the overlap of two-dimensional (2D) projections of the 3D object, however in the weapons counting or discrimination context there are a few pieces of information that we can exploit: general knowledge of certain object dimensions (e.g., external dimensions, shape of internal components) and a very specific task—detection of materials of interest that exceed a specified size. A step toward exploiting the material-discrimination task is examining the use of energy information in radiography to better discriminate special nuclear material (SNM) from benign material or other sources of (background) radiation. This work draws upon the literature in medical imaging and security screening, specifically cargo inspection.

The second image-analysis path relies on generating image transformations that can be used in the creation of templates to verify the presence or absence of weapons or weapons components. The key to such transformations is that they must be non-invertible—destroying the ability to reconstruct details of the original image—yet rich enough in information to enable a confident presence/absence decision. Greater reduction of image information provides greater assurance against possible release of sensitive information, but enough reduction can destroy the ability to verify. In the context of perceptual hashing as a framework for transformations with provable non-invertibility and confident verification, we study the degree of information reduction that maintains verification on a set of test object images using histograms, and consider the question of how to test the ability to reconstruct image details.

The bulk of our work during this first year is summarized in three papers presented at the Institute of Nuclear Materials Management (INMM) Annual Meeting in July 2011. The papers are attached as appendices. In the following report, we briefly highlight the main points and refer the reader to the papers for details. Within this report we summarize our research activity since the INMM meeting.

## 2 Verification Scenarios

Development of verification scenarios, in which objects pertinent to inspection are simulated and analyzed, requires three major tasks: defining the verification objects and their components, surveying the imaging technology available to apply to the components, and generating images that would supply benchmarks for testing and further algorithm development.

### 2.1 Verification Objects

We defined a phased approach in terms of three object-of-interest scenarios. The three scenarios are the AT-400R storage container as used at the Mayak Fissile Material Storage Facility and two nominal nuclear weapons. These objects represent a range of complexity in content, design, and configuration from dismantled components to multiple warheads on a missile. The AT-400R was chosen as a representative dismantlement object currently in use, and because a container is available for imaging at PNNL. Additionally, the general structure of the container and the mass of the fissile material contents of the container are unclassified so that algorithm development, analysis, and results can be carried out and discussed without the need for classified computing or reporting restrictions. Sufficient information on the other objects of interest is available for simulation and subsequent algorithm development and testing on classified systems at PNNL.

### 2.2 Survey of Imaging Technology

We completed a survey of the history of imaging in arms control and radiological imaging technology that might be applicable to warhead verification and counting. The results of this survey were documented in a paper presented at the INMM Annual Meeting in July (see Appendix A). The goal of this survey was to:

- 1) Understand the state of the art in imaging methods and the data/attributes they produce.
- 2) Develop contacts with several of the developers of these imaging systems to allow testing of algorithms with real images.
- 3) Develop a set of requirements for future imaging systems for arms control based on the performance of our algorithms from nominal, multi-modality systems.

From the perspectives of algorithms developed in this project the imaging system would need:

- Sufficient spatial/angular resolution for edge-finding algorithms.
- Photon-counting detectors with sufficient count-rate capability for multi-energy radiography and a materials discrimination algorithm.

We are studying more detailed imaging-system requirements in the context of verification algorithm development, as noted in Section 3.1. Our conclusions in the survey paper included the following.

- Recognizing the breadth of technologies surveyed, it is of interest to combine the algorithms with imaging technology developers to benchmark results with measured data and determine imaging system requirements in terms of algorithm performance.

- Additionally, we currently consider only radiography data. Reconstructing 3D images behind an IB involves more processing and analysis, but the potential benefit may be high verification confidence.
- The perceptual hashing concept may apply to any type of images, but performance in terms of spatial resolution needs to be investigated.

The full survey can be found in the attached paper in Appendix A, and a brief summary of imaging technologies is given in Table 1 of the paper.

An important study not covered in Appendix A is the Project Cloud Gap study performed in the 1960s (declassified in 1999). Figure 2.1 shows one of the main results from Field Test FT-34: Demonstrated Destruction of Nuclear Weapons (Project Cloud Gap). The graph plots the ability of inspectors to discriminate between real and fake weapons versus the intrusiveness of the techniques used (as measured by the number of pieces of classified information revealed during the inspection). The inspection methods were cumulative (e.g., A2 consisted of Geiger counting and the methods in A1). This figure shows that adding x-ray imaging significantly improved the discrimination ability of the inspection, but it also greatly increased intrusiveness. Also of interest is that only full access to the disassembly provided perfect discrimination, but this was not actually tested, just assumed. The challenge of the current project is to demonstrate that the position of point A4 can be moved to the left and possibly up. In other words, to demonstrate that analysis of radiography images behind an IB can benefit verification tasks without compromising information security.

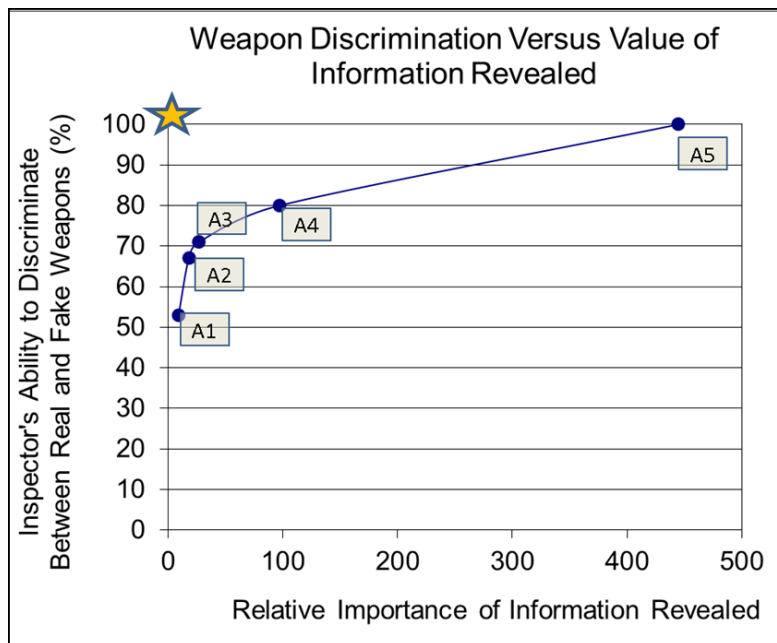


**Figure 2.1. A1: Dimensions, Weights, Centers of Gravity, Case Features, A2: View through Access Doors, Geiger Counter, A3: Neutron Counter and Gamma-spectrometer, A4: X-ray Plate Examination, A5: (untested) Full Access to Weapon Disassembly. The ideal method would be in the top-left corner with 100% discrimination and zero intrusiveness.**

## 2.3 Simulations, Benchmark Images, and Test Images

Simulated radiographs were generated for the AT-400R storage container as well as a number of simple objects for algorithm development. To benchmark the AT-400R simulations we initially measured an available example of the container with its internal contents and a tungsten sphere in place of plutonium, using a 450 kVp bremsstrahlung source and computed radiography plates. The images showed visible contrast between the boundaries of interest and provide confidence that our simulations paralleled reality. Higher-quality images—larger area, higher spatial resolution, and improved contrast—are being pursued using a solid-state, digital imaging system. These data could be used for further simulation benchmarking as well as algorithm testing and development. Details on the other objects of interest were gathered in preparation for simulation, subsequent algorithm development, and testing on classified systems. Further details of AT-400R simulations can be found in Appendix B.

We discussed opportunities to work with images from Oak Ridge National Laboratory (ORNL) staff including Paul Hausladen, Klaus Ziock, John Mihalcz, Seth McConchie, and Brandon Grogan, and were provided with a few representative example results from neutron interrogation-based imaging systems. Many of the ORNL systems have much higher resolution and would be more invasive than those from earlier campaigns such as the “Reentry Vehicle On-Site Inspection (RVOSI) Technology Study” measurements at the FE Warren Air Force Base (Abe, 1994), and represent a potential path forward for application of our techniques. Both unclassified test images and classified data may be available from ORNL from existing and upcoming measurement campaigns. It is our intent to combine our techniques with promising imaging technology. In particular, applying our algorithms to neutron and multi-modal imaging systems such as those developed at ORNL may prove especially fruitful.

## 3 Verification Algorithms

Our image analysis techniques follow two primary paths. The first path broadly considers extracting physical features from radiographic images, such as material composition and attenuation characteristics. These features have been estimated in PNNL's past work by employing assumptions regarding 3D geometric distribution of material, allowing for a limited evaluation of overall density and attenuation characteristics. Research in the first year of the project focused on extending methods developed under LDRD to account for unknown occultation of objects of interest and materials of varying geometry and makeup, while considering that knowledge of the specific geometry will be limited. These results are extended here by considering the energy profile of attenuated photons measured by an active radiography system. The spectroscopic imaging and dual-energy imaging approaches considered by this work can potentially provide a much greater discrimination of SNM from background and other radiological sources. The second image analysis path relies on generating non-invertible transformations of the image to be used as templates for verification, and studying the extent to which such transformations do indeed prohibit the ability to reconstruct details of the original image while enabling confident verification. We studied these questions in the context of "perceptual hashing" as a framework for transformations with provable non-invertibility and confident verification. Ultimately, integration of multiple algorithms is expected to provide the greatest degree of confidence in verification.

### 3.1 Material Discrimination for Attributes

Our progress in development of material discrimination methods and current results is summarized in a paper presented at the INMM Annual Meeting in July, included in Appendix B. The first method is based on multi-energy gamma-ray transmission imaging and the use of mass attenuation coefficients as material basis functions for estimating effective areal densities of individual materials. Limiting the set of basis functions to a set of low-Z materials and Pu, such as would be present in the AT-400R storage container, the method showed promise for correctly indicating Pu where it is present and not indicating Pu where it is absent. These studies assumed a 450-kVp bremsstrahlung source equivalent to an x-ray source available for benchmarking measurements at PNNL. The second method uses spectral images and an energy-window ratio to enhance image contrast and isolate multiple objects in the image. This approach is intended for use in enhancing warhead counting based on passive images.

Our previous efforts on material discrimination hinged on the simplifying assumption that a full image (in principle using either transmission or emission radiography) would exhibit good separation between objects and thereby allow for image verification techniques based on that separation (Robinson et al. 2011). This separation is unlikely in realistic images, due to the unknown and potentially confounding structural elements expected in real objects of interest. However, an imaging system capable of producing images as a function of energy as well as spatial position would have the additional capability of discrimination between regions of interest by using those spectral differences. Incorporating energy information was a key step forward in our methods; combining energy information with limited *a priori* information about object structure is expected to improve discrimination further.

Both spectral methods for contrast improvement and spectral methods as described in the INMM paper, attached as Appendix B, may enhance material discrimination within transmission and emission radiography images. The results from material discrimination approaches can be directly interrogated for

the presence of nuclear materials, allowing for a simple yes/no metric for SNM detection to be developed. Details can be found in Appendix B.

Challenges noted in the paper include accounting for the effects of noise and detecting scattered radiation, which must be studied to begin to make these methods practical. In particular, with dense or thick materials, Compton scattering is expected to produce a substantial number of lower-energy photons which may escape the interrogated object and be detected. High attenuation of gamma-rays in the low-energy region (due to high-Z, high-density materials) combines with the effect of a high level of Compton scattering so that reliable information is limited in the low energy region near the K-edges of the materials. The K-edge features in active radiograph images have been exploited in the past for material discrimination algorithms in the medical imaging field, in which lower-density and lower-Z materials dominate. Excluding low-energy information reduces the dissimilarity between the observed attenuation spectra of different materials, as the K-edges and other distinguishing features are primarily found at lower energies in our initial simulations using a 450 keV endpoint energy source. For example, of the materials studied in the AT-400R container, only the Pu K-edge was included in the analysis due to a choice of lower energy cutoff of 100 keV. Lack of available distinguishing features in the attenuation spectra makes material discrimination more difficult, although current results still suggest SNM discrimination is possible within these limitations.

Our efforts on material discrimination this year since the INMM paper attempt to address some of these challenges, while others will be addressed in the second year of the project.

### **3.1.1 Energy-dependent Passive Image Object Separation**

We designed a set of analyses to demonstrate the use of spectral information to enhance object separation in passive images. Previous passive gamma-ray imaging studied for arms control may not have made full use of spectral information. Incorporating spectral information can help separate sources and allow for verification of objects based on that separation, such as discriminating between background and SNM. The location of interesting regions could then facilitate identification. To demonstrate this potential, we simulated a passive image of the AT-400R containing two spheres of Pu and applied the following spectral contrast enhancement algorithm, the results of which are shown in Figure 3.1. The simulated detector was an ideal pinhole camera situated 2 meters from the object, and two emissive sources were simulated—the Pu objects themselves and a plane of background emissions behind the AT-400R, with spectrum corresponding to previously validated measurements meant to represent the terrestrial background near the PNNL facility. The figure includes a photograph of an example storage container, a simulated passive image, and two stages of results of the algorithm. It should be noted that while many image contrast enhancement techniques exist, our goal is a simple algorithm that can be used within an IB to automatically identify localized SNM sources—images themselves would not be available to any personnel.

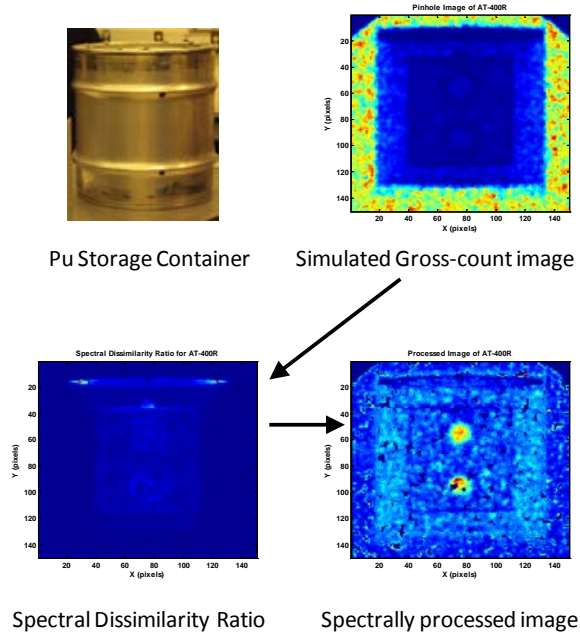


**Figure 3.1. Energy-dependent Passive Image Object Separation**

In many verification measurement settings, it is not likely that a reliable background image containing the object of interest without SNM elements would be available as a basis for comparison. However, we may approximate the unattenuated background  $B(E_k)$  as a function of energy  $E_k$  in a set of energy bins indexed by  $k$  from an image region outside the object. The angle between the vector of counts  $C_{ij}$  in the  $(i,j)$  pixel and the vector of background counts  $B$  (across all energy bins) provides a measure of the spectral difference:

$$M_{ij} = \arccos\left(\frac{C_{ij} \cdot B}{|C_{ij}| |B|}\right).$$

This cosine angle  $M_{ij}$  (labeled “Spectral Dissimilarity Ratio” in the figure) is large in pixels for which background counts are highly attenuated and/or source counts are high, and thus does not itself provide discrimination. Multiplying  $M_{ij}$  by the total intensity in each pixel,

$$A_{ij} = M_{ij} \sum_k C_{ij}(E_k),$$

reveals the two Pu sources as shown in the figure as “Spectrally processed image.” This process can be iterated as the estimate of background is refined, yielding automated object separation/ID in complex images behind information barriers. This example indicates potential for separating sources when background cannot be independently measured, using spectral passive imaging.

### 3.1.2 Analyzing Simple Geometries Consisting of Multiple Materials

The presence of multiple materials is evaluated in this work by considering the energy profile of attenuated photons measured by an active radiography system. To enable a rigorous study of incorporating energy into our material discrimination techniques, and in particular to address the limitations on and determine requirements for these techniques, we stepped back from analyzing the full

AT-400R image to simple geometries with multiple materials. This makes it easier to quantify error in estimation and to understand the limits of our techniques. In this case, a point source with the bremsstrahlung spectrum corresponding to a commercially-available gamma emitter was simulated several meters behind the object to be interrogated, and an ideal plane detector was simulated on the other side of the object to provide image data. Our recent advances address questions associated with noisy images, the use of an extended energy range (source endpoint energy up to 9 MeV) to capture a higher degree of variation in the mass attenuation coefficients of different materials, discrimination between high-Z materials, and the power of combining knowledge of spatial structure with spectral imaging. Many of these advances are aimed at evaluating more realistic data to determine the requirements on imaging systems that can use our techniques, including requirements on measurement time, source energies, and spectral and spatial resolution of the imaging detector.

The problem of material discrimination is cast as fitting the forward (total) attenuation model:

$$C(\bar{E}_j) = C_0(\bar{E}_j) \exp \left[ - \sum_i \mu_i(\bar{E}_j) \rho_i \right]$$

given the mass attenuation coefficients  $\mu_i(\bar{E}_j)$  for materials  $i = 1, 2, \dots, n$  in energy bins indicated by  $\bar{E}_j$  for bins  $j = 1, 2, \dots, m$ , and measured counts  $C(\bar{E}_j)$  in each energy bin. That is, we estimate the areal densities  $\rho_i$  for each material by location (corresponding to each pixel), from which we derive thickness of each material at each spatial location (assuming that the true density is known). This thickness estimate is compared to the true (simulated) thickness of an object to characterize the accuracy of the estimate.

In developing algorithms we drew from a breadth of regression techniques developed largely in the field of chemometrics to solve a similar estimation problem (Beebe et al., 1998). We tested simple linear regression, partial least squares, principle component regression, non-negative least squares (all of the latter on log-transformed data), and a variant of nonlinear optimization, and found non-negative least squares provided the most accurate results. However, the lack of data in the low-energy regions near the K-edges of the materials (due to attenuation and scattering by dense and high-Z materials) precludes the use of those distinguishing features at low energy. Aside from the K-edges, many of the mass attenuation coefficients as a function of E exhibit strong similarity. Any fitting technique would of course be challenged by the near-collinearity of the mass attenuation coefficients in much of the energy range above 100 keV, an example of which is shown in Figure 3.2. Nevertheless, the more pronounced differences between the mass attenuation coefficients of Pu and relatively low-Z materials may enable confident discrimination between low-Z and SNM materials.

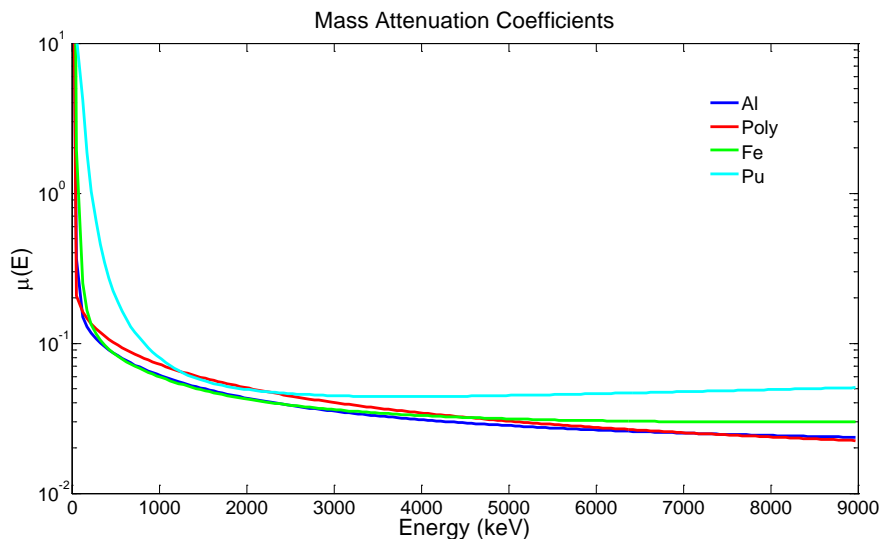


**Figure 3.2. Mass Attenuation Coefficients of Four Materials Used in the AT-400R Storage Container. Total cross-sections were obtained from the ENDF cross section libraries from the National Nuclear Data Center.**

### 3.1.2.1 Implementing the Algorithm

Following submission of the INMM paper on material identification, work has focused on three questions:

1. Effects of noise: Unsurprisingly, the basis-function decomposition works well to identify materials in noise-free simulations (that do not contain scattered radiation). We have begun work on models that incorporate photon noise, and for highly attenuating objects (e.g., Pu) in the energy range considered, the fits are qualitatively much worse than in the noise free case. We are developing metrics to quantitate the degradation in the ability to identify materials by the inversion algorithm as a possible direction for determining minimum flux at the detector (and thus imaging times).
2. Incorporating spatial-structure constraints: Inversion to determine materials in the object in the work described above was performed on a pixel-by-pixel basis. However, it is possible that information about the spatial structure of objects of interest may be available and could be incorporated in the inversion. In a dismantlement scenario, spatial structure may be known quite well, and that information could be used to simplify the problem of determining whether a specific fissile material is present in a declared amount. In a warhead verification scenario, constraining the problem with even a limited knowledge of structure is likely to make a big difference. Additionally, spatial information can be learned behind an information barrier by drawing from the wealth of edge- and shape-finding image analysis tools, and then used to constrain material discrimination. We have had some success improving the results of the inversions of noisy simulations by applying constraints on the number of materials that can contribute to a region of the image.
3. Determining optimal energy regions: This is a two-pronged attack that has examined the uniqueness of the basis functions (mass attenuation coefficients) used as a function of energy, and

an empirical study of inversion results using bremsstrahlung sources of different end-point energies. Results of this work are expected to help determine the requirements for an X-ray source (and detector) needed for the inversion algorithm to be successful.

### **3.1.2.2 Additional Areas of Study**

Further study is needed to determine optimal energy regions in terms of two objectives: minimizing the collinearity of material mass attenuation coefficients and maximizing signal.

Work in the second year of the project will focus on developing a framework for determining imaging system requirements for our verification algorithms and providing requirements for example imaging systems and verification problems, while continuing to improve the algorithms by incorporating more realistic noise models, realistic spatial structure constraints for more complicated structures, testing, and renewed development on simple layered material models, the AT-400R model, and unclassified models of objects similar in structure to nuclear weapons. Merging of spectral and spatial approaches to material discrimination will also be performed, specifically exploiting the existing image analysis algorithms for edge finding and shape estimation. Discrete image region finding will be combined with constraints on differences in composition between regions (e.g., the idea that one edge in an image only represents one change in material composition) in order to arrive at a powerful material discrimination approach.

## **3.2 Non-invertible Transforms for Templates**

We initiated a study of the perceptual hash for image reductions as a provably non-invertible transformation. The concept may provide the framework needed to address concerns about the histogram comparison approach we studied for dismantlement verification (Robinson et al. 2011). Perceptual hashing methods use the core idea in cryptographic hashing but were developed to allow matching between images that are identical but for small variations (e.g., scaling, rotation, compression). These methods are being studied to develop a template approach that greatly reduces the risk of disclosing sensitive information contained in images and the attributes that are extracted from them. Perceptual hashing was developed for multimedia content authentication, image tampering detection, and image database search. It combines image reduction techniques, like the histogram, with hash functions to provide compact representations of images for comparison. Several references for perceptual hashing can be found in Appendix C. Reduced images (e.g., features) must be coarse enough so that images that are perceptually the same are declared a match. We summarized the challenges of sensitive information protection for application of the histogram comparison technique, and the proposed use of perceptual hashing to address these challenges, in a paper presented at the INMM Annual Meeting in July.

The perceptual hash can incorporate and enhance the histogram approach, and may incorporate any alternative methods for image reduction. While some excellent results have been obtained for the perceptual hash in different applications, an ability to simultaneously verify declared items and protect sensitive information in inspection settings must be demonstrated in principle. The appeal of implementing a perceptual hash concept lies primarily in its reliance on well-established cryptographic hash results, and the acceptance of hashing in IB technology. In terms of comparison to a reference, conceptually the process can be thought of in terms of comparing either the original images or a specific reduction of those images. A perceptual hash could also be applied to any attributes derived from images based on physical principles and result in a template derived from agreed-upon attributes. In any case, perceptual hashing may allow templates to be used without the need to store sensitive data. Thus the

perceptual hash concept has potential broad application for enabling imaging in arms control. Details of our summary of challenges of sensitive information protection and the potential use of histogram comparison in a perceptual hash framework can be found in the paper attached as Appendix C.

Histograms and many other transformations of images are, strictly speaking, not invertible—one cannot reconstruct the original image from the transformation alone. However, *a priori* knowledge or expectation of structure in the image helps constrain the inversion, so that image reconstruction may be possible. Further reduction of information in the transformation (e.g., coarsening histograms) makes reconstruction more difficult, but also can hinder verification when comparing transformed images of reference and observed objects.

Two fundamental questions arise:

- How much structural knowledge is enough to reconstruct details, and
- How can one reduce information or selectively introduce artificial noise to defeat inversion while maintaining confident verification?

After the INMM paper, we initiated a study of the latter question and proposed a pathway for studying the former. As an example of data reduction to defeat inversion, we considered coarsened histograms as described below.

### 3.2.1 Tuning Data Reduction to Achieve both Verification and Information Protection

To study the effect of coarsening on verification confidence and protection of sensitive information, we define information reduction parameters and try to determine parameter values that maximize confidence and minimize the possibility of inversion. Our version of histogram coarsening is defined in terms of the number of intensity bins taken as  $2^k$  for varying integer  $k$  values and quantization of frequencies by multiples of  $2^l$  for varying integer  $l$  values. Figure 3.3 shows an example of a histogram with maximal number of bins and frequency-quantization levels along with a coarsened version of the same histogram, using fewer bins and frequency quantization levels. The goal is to reduce information until coarsened histograms of images of the same object are identical or nearly so, while keeping enough information so that coarsened histograms of images of different objects are significantly different.

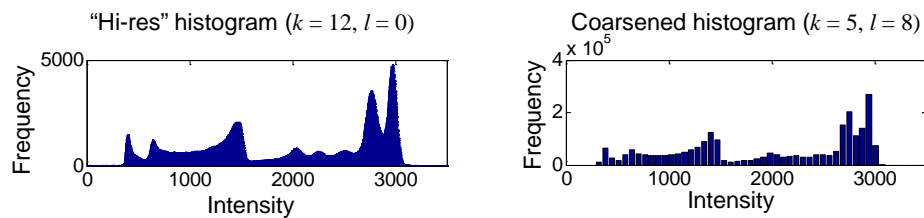


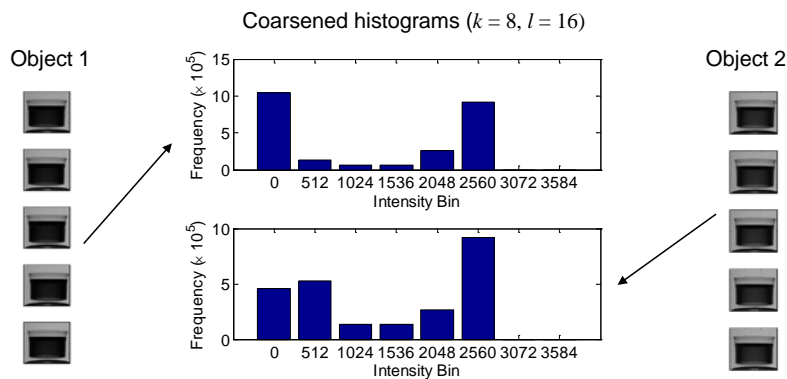
**Figure 3.3. Histogram Coarsening Defined by Number of Intensity Bins and Quantization of Frequency Levels**

Cumulative coarsened histograms  $C_i$  (simply defined as the cumulative sum over bins) are used within a Euclidean distance  $d_{ij} = \|C_i - C_j\|_2$  for images  $i$  and  $j$  to quantify difference between the two images. When comparing two images in this way, achieving an exact match on images of the same object and no match on images of different objects is ideal for verification. At some level coarsening will eventually

result in exact match between any two coarsened image histograms, destroying the ability to verify. One of the key questions is whether parameter values exist that provide the ideal result. Short of the ideal, we may consider optimizing parameter values with the dual objective of minimizing distances  $d_{ij}$  between images of the same object and maximizing distances between images of different objects.

We test an approach to this optimization on a set of ten images drawn from our previous LDRD effort (Robinson et al., 2011). Figure 3.4 shows the images, which were generated by the gamma-ray transmission imaging system described in that paper. The objects are two Marinelli beakers filled with epoxy of two different densities, shifted around in the field of view of the imaging system to create some variation in addition to measurement error/noise. We tested a simple objective function that may be considered a “distance between the distances”: the set of distances  $d_{ij}$  between images of Object 1 is compared to the set of distances between images of Object 1 and Object 2 in terms of the means of each set, normalized by the variance of the set of Object 1 distances (akin to a Mahalanobis distance).

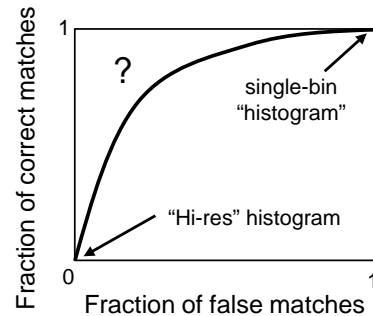
Alternatively, the fraction of exact matches in each group of comparisons may be used as a basis for determining optimal parameters. Figure 3.5 shows results in our test case, in which parameter values can be found such that the verification ideal is achieved: at these parameter values, all of the coarsened histograms of Object 1 match exactly, and none of those matches the coarsened histograms of Object 2.



**Figure 3.4. Histogram Comparison: Effect of Coarsening on Verification with the Marinelli Beaker Test Case**

In cases with more realistic images for treaty verification, the notional tradeoff curve shown in Figure 3.5 may be used to quantify verification confidence in terms of correct and false matches as a function of coarsening parameters. A correct match here means that two images of the same object are correctly declared as such; a false match means that two images of different objects are incorrectly declared as images of the same object. The curve indicates that at high levels of coarsening, the fraction of both correct and false matches is high, with the extreme case of a single histogram bin (giving the total number of pixels) producing a match for any two images; likewise low levels of coarsening produce few matches in either case.

Notional Histogram-based Verification Curve

**Figure 3.5. Notional Histogram-based Verification Curve**

The critical follow-on question is whether we also have a non-invertible transform at a point on the curve in Figure 3.5 that represents an acceptable level of verification confidence. To put it bluntly, is there any point on the curve for which sensitive information cannot be extracted from the histogram? To try to provide a defensible answer to this question, we propose that a set of designed experiments with a simulated intelligent adversary is needed to test the invertibility of the histogram process. This could entail collaboration with existing vulnerability assessment groups, or development of such a group in future efforts. For example, either an internal or external team could be set up to attack the histogram comparison approach, by modeling the histogram as a function of structural/material parameters and determining whether accurate parameter estimates representing sensitive information can be obtained. With the transmission images of Marinelli beakers, features in the histograms can be roughly mapped back to the areal density of the material in the beakers at different locations. By modeling attenuation using beaker density, cylinder radii and heights as parameters, can the beaker details be reconstructed? Then we can determine the level of information reduction at which the histogram process is not invertible to a degree sufficient to reveal sensitive information. This would establish a framework for such studies on more realistic images. Additional remaining challenges include laying the mathematical and empirical analysis foundations to address information management, robustness, and verification requirements.

The steps above outline a framework for studying verification confidence that fits within the perceptual hashing paradigm. Implementations and tests of the perceptual hash in other contexts have included methods for rigorously quantifying the accuracy of matching images in spite of slight variations, as well as rigorously quantifying the potential for invertibility of the perceptual hash such as the coarsened histogram.

## 4 Conclusions

In this first year of the project, we began by surveying the imaging technology and defining a set of prototype problems and imaging scenarios. We refined the techniques developed under the previous LDRD investment, in particular by considering increasing realism in a variety of ways. The AT-400R container represents a more realistic object of interest as a basis for development, with multiple materials in layered, more complex geometries than we studied previously.

Further refinement of material discrimination methods is needed to understand its limits with realistic images and to define imaging system requirements. In particular, the potential improvement in discrimination by combining geometry and structure assumptions into regression models must be quantified for realistic images. The applicability of these techniques must be broadened to take advantage of a variety of recently developed systems such as combined neutron-gamma radiography systems under development at CSIRO in Australia. Such systems hold the potential for improving our techniques as well, by providing dual-mode information that can help discriminate materials.

We studied coarsening in the histogram comparison technique as a form of perceptual hashing to generate a non-sensitive template, outlining a simple approach for quantifying the verification confidence as a function of coarsening parameters. Rigorous mathematical foundations for the use and study of robustness and security of the histogram comparison and related perceptual hashing techniques must be developed using an extended set of realistic images, and taking advantage of perceptual hashing analysis in other applications.

We will continue to develop techniques with the following fundamental verification challenges in mind. Attributes derived for material discrimination are intended to be non-sensitive, and the perceptual hash is intended to be a non-sensitive reduction of an image, so that both can be stored outside an IB. Figure 4.1 shows a schematic of the intended integration of perceptual hashing with IBs as an example. The question is whether sensitive parameters can be determined from the attributes or from the perceptual hash. If not, then storing these as references may be acceptable, making imaging for warhead verification possible. Otherwise, alternative approaches will need to be explored. We propose that determining the answer to this question requires developing an adversarial attack strategy, perhaps using an independent team, to assess the vulnerability of our techniques.

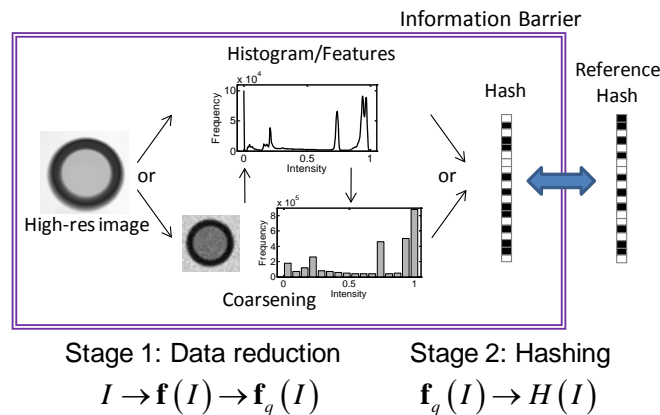


**Figure 4.1. Creating a Non-sensitive Reduction of the Image**

In the following two years of the project, we plan to finalize further refinements to the techniques, demonstrate the integration of the techniques with formal IB principles, test the techniques on images taken in laboratory and campaign settings (as available), and analyze their performance.

## References

- Pitts WK, KD Jarman, EA Miller, BS McDonald, AC Misner, MJ Myjak, SM Robinson, A Seifert, CE Seifert, and ML Woodring. 2010. "Advantages of dual mode imaging for managing sensitive imaging information." In Proceedings of the 51st Annual Meeting of the Institute of Nuclear Materials Management, July 11-15, 2010, Baltimore, Maryland. INMM, Deerfield, IL. PNNL-19546.
- Robinson SM, KD Jarman, EA Miller, AC Misner, MJ Myjak, WK Pitts, A Seifert, CE Seifert, and ML Woodring. 2010. "Image analysis algorithms for dual mode imaging systems." Proceedings of the 51<sup>st</sup> Annual Meeting of the Institute of Nuclear Materials Management, July 11-15, 2010, Baltimore, Maryland. INMM, Deerfield, IL. PNNL-SA-73315.
- Robinson SM, KD Jarman, WK Pitts, A Seifert, AC Misner, ML Woodring, and MJ Myjak. 2011. "Imaging for dismantlement verification: information management and analysis algorithms." PNNL-SA-78495, Pacific Northwest National Laboratory, Richland, WA. [Accepted for publication in *Nucl. Instrum. Methods Phys. Res. A*.]
- McDonald B.S., A. Seifert, T.A. White, S.M. Robinson, E.A. Miller, K.D. Jarman, A.C. Misner, and W.K. Pitts, "Image-Based Verification: Some Advantages, Challenges, and Algorithm-Driven Requirements," Proceedings of the Institute for Nuclear Materials Management 52nd Annual Meeting, July 2011, Palm Desert, CA.
- Jarman KD, SM Robinson, A Seifert, BS McDonald, AC Misner, TA White, EA Miller, and WK Pitts, "Non-Invertible Transforms for Image-Based Verification," Proceedings of the Institute for Nuclear Materials Management 52nd Annual Meeting, July 2011, Palm Desert, CA.
- Robinson SM, KD Jarman, A Seifert, BS McDonald, AC Misner, TA White, EA Miller, and WK Pitts, "Image Based Verification Algorithms for Arms Control," Proceedings of the Institute for Nuclear Materials Management 52nd Annual Meeting, July 2011, Palm Desert, CA.
- Beebe, KR, RJ Pell, and MB Seasholtz. 1998. Chemometrics: A Practical Guide. Wiley Interscience.
- U.S. JOINT DOD-DOE INFORMATION BARRIER WORKING GROUP. 1999. Functional Requirements for Information Barriers. Pacific Northwest National Laboratory, Richland, WA. PNNL-13285.
- M. C. Abe, 1994. "Reentry Vehicle On-Site Inspection Technology Study," DNA-TR-94-22, Defense Nuclear Agency.

**Appendix A: Image-based Verification: Some Advantages,  
Challenges, and Algorithm-driven Requirements  
(PNNL-SA-80551)**

## IMAGE-BASED VERIFICATION: SOME ADVANTAGES, CHALLENGES, AND ALGORITHM-DRIVEN REQUIREMENTS

**Benjamin McDonald**<sup>\*</sup>, Allen Seifert, Timothy White, Sean Robinson, Erin Miller,  
Kenneth Jarman, Alex Misner, William K. Pitts.

Pacific Northwest National Laboratory (PNNL), Richland, WA, 99352 USA

### ABSTRACT

Imaging technologies may provide particularly useful techniques that support monitoring and verification of deployed and non-deployed nuclear weapons and dismantlement components. However, protecting the sensitive design information requires processing the image behind an information barrier and reporting only non-sensitive attributes related to the image. Reducing images to attributes may destroy some sensitive information, but the challenge remains. For example, reducing the measurement to an attribute such as defined shape and X-ray transmission of an edge might reveal sensitive information relating to shape, size, and material composition. If enough additional information is available to analyze with the attribute, it may still be possible to extract sensitive design information. In spite of these difficulties, the implementation of future treaty requirements may demand image technology as an option. Two fundamental questions are raised: What (minimal) information is needed from imaging to enable verification, and what imaging technologies are appropriate? PNNL is currently developing a suite of image analysis algorithms to define and extract attributes from images for dismantlement and warhead verification and counting scenarios. In this talk, we discuss imaging requirements from the perspective of algorithms operating behind information barriers, and review imaging technologies and their potential advantages for verification. Companion papers will concentrate on the technical aspects of the algorithms.

### INTRODUCTION

Future nuclear arms reduction treaties may require precise counting of warheads. How this will be implemented is an open technical and political debate. Imaging technologies, which elucidate both form and function, may be among the best tools for warhead verification. For instance, imaging may be best for discriminating between fissile materials in a weapon form versus rubble. PNNL is developing algorithms that extract attribute information from images behind an information barrier (IB). We are exploring ways to process images so that sensitive data is protected and never stored behind the IB. Imaging for warhead verification has never been implemented because it is so intrusive, but this is also what makes it so useful [1]. New imaging technology may help solve challenging verification problems that might not be solved otherwise without complete, unfettered access to the warhead. We aim to show the utility *and* practicality of imaging with low-intrusion image-processing algorithms operating behind an IB.

<sup>\*</sup>Corresponding Author: tel: (1) 509.375.1872, email: benjamin.mcdonald@pnnl.gov

### IMAGING IN ARMS CONTROL & DISMANTLEMENT VERIFICATION

The history of imaging in arms control is fairly succinct: flat-out rejection for consideration in warhead counting due to excessive intrusion. Nevertheless, several groups have assessed the possibilities.

Both the Soviet Union and the USA had compelling reasons to forge the Intermediate-Range Nuclear Forces (INF) treaty, which led to unprecedented intrusive inspection measures. Imaging was used in two ways in the verification of the INF Treaty. First, to establish that only SS25 missiles (and not SS20) were leaving the Votkinsk missile facility in Russia, a 9 MeV Linatron x-ray radiography system was used to scan rail cars (with missiles inside) as they left the facility. Warheads were not imaged, but other features of the missiles that were dissimilar (length and width) were determined using imaging [2]. Another feature of the INF treaty was short-notice, on-site inspections, where the neutron flux from a missile was mapped. An inspector used a hand-held neutron counter for measurements along a grid laid on the floor (effectively creating a coarse-resolution image):

“A launch canister with a missile inside containing a single warhead (SS-25) emitted a different pattern of fast neutrons than did one with a missile having three warheads (SS-20). The American inspection team, using the RDE (radiation detection equipment), compared their measurements against a set of benchmark radiation measurements taken during a special inspection in the summer of 1989. [2]”

While these inspections (and visual inspections of RVs) continued, the U.S. considered technology alternatives and issues for warhead counting [3]. The “Reentry Vehicle On-Site Inspection (RVOSI) Technology Study” aimed to rank available technologies based on confidence, intrusiveness, cost, inspector burden, and operational impact. Most of the technologies surveyed were passive radiation (neutron or gamma-ray) imaging techniques, as they were the most developed. Compton imaging was only just finding applications outside of gamma-ray astronomy, and x- or gamma-ray radiography was considered too intrusive and not included in the study. That left coded apertures, neutron counting systems, collimated detectors, and a few active interrogation methods. Scanning geometries and measurement scenarios were considered. The top pick of the study was the Gamma-Ray Imaging System (GRIS) [4, 5] from LLNL, as it had the most use in field measurements, simpler, end-on-geometry and the highest confidence in correctly counting warheads.

Researchers at the Atomic Weapons Establishment in the UK considered imaging techniques for a dismantlement verification project, including thermal imaging, radiography, and neutron counting [6]. Because of the invasiveness of these methods, it was concluded that “national security and proliferation concerns will probably mean that such ‘unfiltered’ techniques will be of limited use in a verification regime without information security barriers [6].” Issues with verifying an operational weapon versus a dismantlement component are noted as well:

“The challenge associated with authenticating a fully assembled thermonuclear warhead, of unknown design complexity and potentially mated to a carrier or reentry vehicle, is far greater than authenticating a warhead’s fissile pit or material in a transport or storage container [2].”

Inspector confidence and technology intrusiveness have suffered an inversely proportional relationship for consideration in warhead counting. If the intrusiveness of imaging is sufficiently mitigated by operating behind an IB, then its use in a verification regime may be more easily accepted. A key aspect of the success may be jointly developed imaging hardware and imaging algorithms [7]. With low-intrusion algorithms we aim to enable imaging as a highly useful tool in challenging verification scenarios.

### LOW-INTRUSION ALGORITHMS

In 2010 we presented three low-intrusion algorithms [1, 8] which showed promise for simple objects. This year we are developing techniques in two broad areas, which are described in more detail in companion papers [9, 10]. In short, we examined the concept of using a ‘perceptual hash’ to protect image data (Fig. 1) and multi-energy methods for material discrimination (Fig. 2).

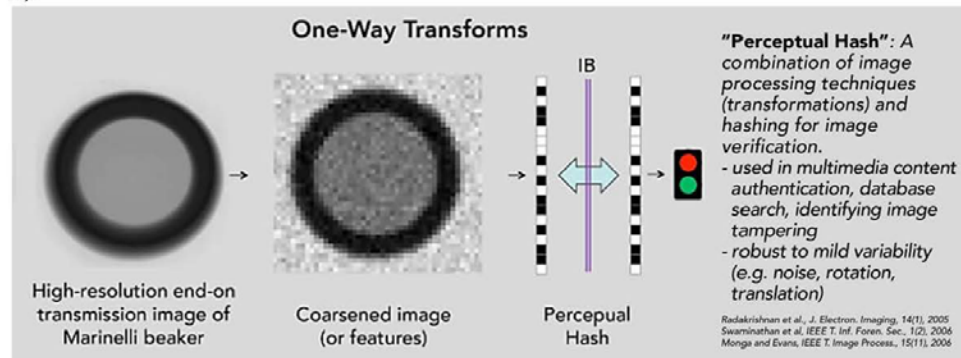
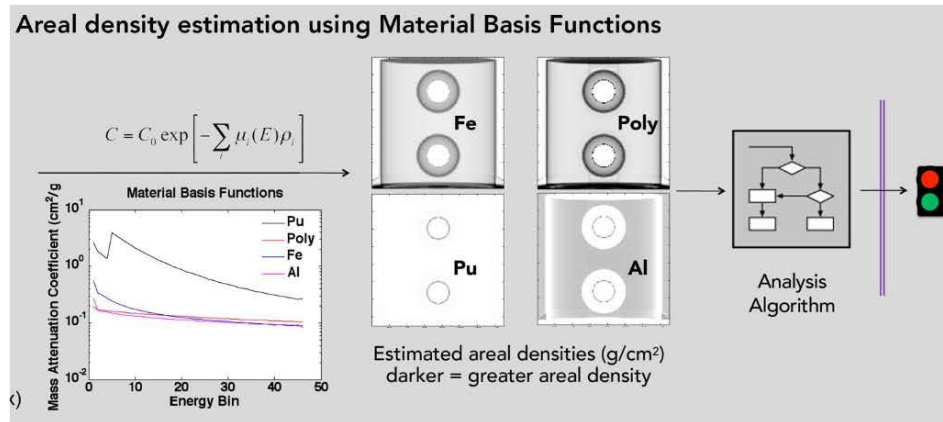


Figure 1: Overview of perceptual hash concept. More details are in a companion paper [9].

One-way transforms (such as hashes) are a way to protect sensitive information and transfer it out of the IB [11, 12]. However, no two images will ever be exactly the same, thus standard hashes of those images will differ. The perceptual hash might be a way to compare several images of the same item taken under slightly different conditions (e.g., viewing angle) and give the same hash output. It could thus be used on image data from any source for verifying attributes within a certain range or comparing against a measured template (in which only the hash result would be stored).



**Figure 2:** Overview of areal density estimation from material basis functions and a simulated AT-400R container. By using a Bremsstrahlung source and a photon-counting detector, materials in a radiograph may be distinguished. More details are given in [10].

Spectral methods may permit material discrimination and enhance previous attempts to discern materials within active and passive radiography images. Some material discrimination approaches easily show the presence of nuclear materials, allowing for a simple detection metric for SNM presence to be developed. These methods may prove useful for the verification of objects in both warhead counting and dismantlement regimes.

## REVIEW OF IMAGING TECHNOLOGIES

We surveyed the open literature on imaging technologies that had been developed or proposed for arms control verification. Nuclear and radiological systems were of primary consideration, and within this broad category we focused almost entirely on systems that rely on direct emissions or transmissions. Several recent reports summarize the state of the art in image formation methods (e.g., [13, 14]), thus, only the salient features of individual imaging systems are described. A host of mature and emerging technologies could be applicable to warhead counting, including some non-radiological methods (e.g., thermal imaging). A limited, neutral survey of the field is given in Table I.

## PASSIVE IMAGING

Any signal emanating from a warhead can be used to help identify the source materials. However, there may be very little signal coming out of the object depending on the shielding. Passive technologies may be summarized in terms of the following five groups.

**Fast-neutron scatter cameras:** [15, 16]. SNL's camera detects and distinguishes fast neutron interactions and gamma-rays with two planes of liquid scintillator detectors. Pulse shape analysis permits discriminating between gamma-rays and neutron interactions. Based on the interaction

position of the scatter in the front and back plane and the time between the events, the direction of the neutron can be confined to a conical shell. Images are created by processing (using backprojection or iterative reconstruction algorithms) the list-mode data which contains timing and energy information.

**Coded Apertures (Gamma-ray):** These consist of a patterned mask of attenuating material (many pinholes), a position-sensitive detector, and a deconvolution scheme [17]. They are generally most efficient for imaging sources with energy below 500 keV, above which it becomes challenging to create sufficiently attenuating masks. These systems have a long history in astronomy (imaging point sources in the sky) and a mixed history in medical imaging (where sources are often distributed and in the near-field). Their demonstrated performance in arms control verification tests is noteworthy (e.g., OSL Coded aperture (PNNL) [18, 19] and GRIS (LLNL) [4, 5]). Instead of a coded aperture, a simple pinhole or parallel-hole collimator can be used. These have lower efficiency, but do not require a deconvolution scheme since the object projections from each hole do not overlap. Such a gamma-camera (Anger camera) with a honeycomb collimator was jointly developed by Russian and US scientists in the late 1990s to determine a shape attribute of fissile material [20].

**Coded Aperture Cameras (Neutron):** For thermal neutrons the mask is made of cadmium [21]; for fast neutrons the coded aperture is poly [22]. Both of these could be useful in warhead counting for verification of different attributes.

**Compton cameras:** These have better performance for gamma-rays with energy above 300 keV. Two detector planes are generally required (ideally the photon scatters in the first plane and the scattered photon is absorbed in the second plane). The interaction positions and the energy depositions make it possible to define a cone of angles from which the photon originated. An example high-resolution system was made by Burks at LLNL [23].

**Hybrid (Coded aperture + Compton):** These systems extend the energy range for imaging efficiency. A combined system better utilizes the expected range of photon energies emitted from special nuclear materials. The High Efficiency Multimode Imager (HEMI) uses an active mask coded aperture, which doubles as the scattering plane in a Compton camera and as an attenuating mask for a coded aperture system [24].

#### **ACTIVE IMAGING (TRANSMISSION, REFLECTION, OR INDUCED)**

Active imaging systems require that a radiation source (x-ray tube, Co-60 source, DT head, etc.) irradiates the object of interest and that a detector records the resulting signals. These systems may be broken into categories by source type.

**X- or gamma-ray radiography:** The CoLOSSIS system is an accelerator-based x-ray computed tomography (CT) system for high-resolution inspection in stockpile stewardship activities [25]. This machine produces a 9 MeV Bremsstrahlung beam and includes a lens-coupled CCD detector that offers higher spatial resolution than would probably ever be needed for arms control verification. Systems using lower-energy x-rays and off-the-shelf components (e.g., 450 kVp industrial x-ray tube with a flat panel integrating detector) may be sufficient to determine a symmetry attribute. For highly shielded objects, high-resolution MeV imagers that are being

developed for cargo scanning (e.g. [26]) may find use in arms control. Such imaging systems may be similar to the INF scanner, but perhaps with energy-resolved detectors.

**Neutron radiography:** Associated particle sealed-tube neutron generators can be used to scan a missile on its circumference and gain isotopic information about the contents from fission gamma rays or density/material information from neutron attenuation [27]. The Nuclear Materials Identification System (NMIS) and the Advanced Portable Neutron Imaging System (APNIS), both tomographic imagers, can produce several types of images (transmission, induced fission, and induced neutron pairs [22, 28-31]). These systems have the ability to create density maps with the neutron transmission data and overlay them with estimates of SNM-containing regions from the induced fission data.

**Table I:** Neutral survey of imaging technologies and example systems.

Mode	Imaging Technique	Example Imaging System
Passive	Compton imaging	LLNL, M Burks, Si + HPGe planes [23]
	Gamma-ray coded aperture	LLNL, K Ziock, GRIS [5]; PNNL, S Miller, OSL [19]
	Thermal neutron coded aperture	BNL, PE Vanier, Cd aperture [21]
	Fast neutron coded aperture	ORNL, Blackston & Hausladen [22]
	Fast neutron double-scatter camera	SNL, N Mascarenhas [16]
	Thermal imaging	ORNL & others, [32]
	Hybrid Compton/coded aperture	LBNL-UC Berkeley, PN Luke, HEMI [24]
	Time projection chamber	LLNL, N Bowden [33]
Active (transmission)	X- or gamma-ray radiography	LLNL, Colossis [25]; ANL, Gamma hodoscope [34]
	Associate particle neutron radiography	ANL, Hodoscope [35]
Active (induced)	Induced Fission Mapping	ORNL, JT Mihalcz, NMIS [28]
Multi-modal	Emission/transmission CT (photon)	Waste drum scanners: LLNL, WIT [35]; LANL, TGS [36-38]
	Passive/active neutron imaging	ORNL, Blackston & Hausladen [22]
	Neutron-photon radiography	CSIRO, B Sowerby, FNGR [39]
	Coded aperture + LIDAR	ORNL, K Ziock [40]

#### MULTI-MODALITY IMAGING SYSTEMS

**Fast neutron and gamma-ray radiography (FNGR):** FNGR measures the ratio of fast neutron and gamma-ray mass attenuation coefficients, which gives the average material composition in the beam independent of the mass of the material [39]. A commercial system is being tested at Brisbane International Airport [41].

**Gamma-ray + LIDAR:** HPGe strip detectors and a coded aperture with laser scanning (LIDAR) were combined in [40]. LIDAR gives 3D (surface) scene information. The advantage of the LIDAR data is clear in holdup scenarios with varied backgrounds, but probably has limited utility in a warhead counting or dismantlement scenario, where everything is behind a shroud or other purposeful concealment.

**Combined Emission/Transmission Computed Tomography:** Tomographic Gamma Scanning (TGS), developed by at LANL and commercialized by Canberra, uses a radioisotope source to

perform a transmission scan of a waste drum, which is then used to perform attenuation-correction on passive gamma-ray images [42-44]. Waste Inspection Tomography (WIT), developed by LLNL & Bio-Imaging Labs, LLC, uses active and passive computed tomography (emission images are attenuated-corrected by transmission data as in the TGS system) [36-38]. WIT is implemented on a semi-truck and uses a Linac to perform transmission scans. Both show the utility of combining active and passive data.

Photon transmission imaging allows access to attenuation coefficients ( $Z$  and density), and possibly elemental ID if we consider the K-edges; neutron transmission radiography might allow material ID, but in general has no better material ID capability than photon radiography, although the cross-section info may be complementary [39]. In comparison, photon/neutron-induced signatures identify material. Passive emission signatures (photon/neutron) identify material but are dependent on inherent shielding properties. Thermal imaging may indicate presence of radioactive material. Choice of signature will have to consider the other material in the object that may have confusing or obfuscating properties.

### IMAGER REQUIREMENTS

What imager requirements are needed to ensure top algorithm performance? This is a broad question that is highly dependent upon the object type and geometry of the measurement. We can, however, make the following general statements:

- Multi-modal systems can provide complementary information which theoretically increases confidence in warhead counting scenarios (more attributes, better spoof detection)
- Induced signals may be acquired from more flexible geometries (require access to only one side of object), but require longer acquisition times ( $1/r^4$  instead of  $1/r^2$  geometric efficiency).
- Task-based performance is the best metric: e.g., how well does the imager count warheads?
- Imaging algorithms and the IB should be jointly developed [7].

For a specific scenario, we can search for the technologies that provide acceptable tradeoffs between the competing demands of (in a proposed descending order of importance) [45]:

- Confidence in the result (transparency and verification), including spoofing detection;
- Protection of classified information (inherent imaging system obfuscation, e.g. to produce poorer resolution than is possible, may not be needed with the right algorithms);
- Time of measurement;
- Cost; and
- Operational robustness.

In the past, efforts have been made to mechanically limit the intrusiveness of the monitoring/verification system by purposefully reducing the spatial or energy resolution of the system (e.g., [46]). Another idea is to keep the coded aperture obscured, making the image-unfolding process nearly impossible [19]. On the other hand, if there is great confidence in the IB, more resolution likely means increased algorithm performance. From the perspectives of algorithms developed in this project the imager would need:

- Sufficient Spatial/Angular resolution for edge-finding algorithms.

- Photon-counting detectors with sufficient count-rate capability for multi-energy radiography and materials discrimination algorithm.

### CONCLUSIONS & FUTURE WORK

We are developing image-processing algorithms for attribute verification behind an IB to mitigate potential intrusion concerns and enable imaging technologies for arms control. The perceptual hash represents promising route to this end, and the material basis algorithm should enhance the utility of transmission radiography. The algorithms are intended to be nominally independent of specific imaging systems. Recognizing the breadth of technologies outlined here and many more not included in this outline, it is of interest to combine the algorithms with imaging technology developers to benchmark results with measured data and determine imager requirements in terms of algorithm performance. Combinations of algorithms and multi-modal systems may prove especially fruitful, and further study on what can be achieved by combining nuclear and non-nuclear (e.g., resonant ultrasound [47] and induced eddy current [48]) techniques in terms of attribute verification is needed [45, 49]. Additionally, we currently consider only radiography. Reconstructing 3D images behind an IB involves more processing and analysis, but the potential benefit may be high verification confidence.

### ACKNOWLEDGEMENTS

This research is supported by the U.S. Department of Energy National Nuclear Security Administration Office of Nonproliferation and Verification Research and Development. The Pacific Northwest National Laboratory is operated by Battelle for the U.S. Department of Energy.

### REFERENCES

- [1] A. Seifert, K. Jarman, E. Miller, A. Misner, M. Myjak, W. Pitts *et al.*, "Imaging for Dismantlement Verification: Information Management and Analysis Algorithms," PNNL-19824, Pacific Northwest National Laboratory (PNNL), Richland, WA (US), 2010.
- [2] J. P. Harahan, *On-Site Inspections Under the INF Treaty, A History of the On-Site Inspection Agency and Treaty Implementation, 1988-1991*: Treaty History Series, Government Printing Office, 1993.
- [3] M. C. Abe, "Reentry Vehicle On-Site Inspection Technology Study," DNA-TR-94-22, Defense Nuclear Agency, 1994, p. 114.
- [4] T. B. Gosnell, J. D. Cole, B. D. Geelhood, S. D. Miller, H. L. Scott, and K. P. Ziock, *Warhead-Counting Demonstration for RVOSI by Department of Energy Laboratories*, JEP-001, Lawrence Livermore National Laboratory, 1992.
- [5] K. P. Ziock, C. J. Hailey, T. B. Gosnell, J. H. Lupton, and F. A. Harrison, "A gamma-ray imager for arms control," *IEEE Transactions on Nuclear Science*, vol. 39, no. 4, pp. 1046-1050, 1992.
- [6] G. J. George, Ley, M.D. , "Nuclear Warhead Arms Control Research at AWE," *Verification Yearbook*, T. Findlay and O. Meier, eds., p. 227, London: VERTIC, 2001.
- [7] M. R. Smith, J. Dunn, and K. Seager, "Future directions for arms control verification technologies," in *Proceedings of the Institute of Nuclear Materials Management Annual Meeting*, Baltimore, MD, 2010.
- [8] S. Robinson, K. Jarman, E. Miller, A. Misner, M. Myjak, W. Pitts *et al.*, "Verification Algorithms for Dual Mode Imaging Systems," in *Proceedings of the Institute of Nuclear Materials Management Annual Meeting*, Baltimore, MD, 2010.
- [9] K. Jarman, S. Robinson, A. Seifert, B. S. McDonald, A. Misner, T. White *et al.*, "Non-Invertible Transforms for Image-Based Verification," in *Proceedings of the Institute of Nuclear Materials Management Annual Meeting*, Palm Desert, CA, 2011.

- [10] S. Robinson, Jarman, K., Seifert, A., McDonald, B., Misner, A., White, A. Miller, E.A., Pitts, W.K., "Image-Based Verification Algorithms for Arms Control," in Proceedings of the Institute of Nuclear Materials Management Annual Meeting, Palm Desert, CA, 2011.
- [11] R. R. Hansen, R. B. Bass, R. T. Kouzes, N. Mileson, P. N. N. Laboratory, and U. S. D. T. R. Agency, "Implementation of the AES as a Hash Function for Confirming the Identity of Software on a Computer System," PNNL-14170, Pacific Northwest National Laboratory, 2003.
- [12] A. J. Menezes, P. C. Van Oorschot, and S. A. Vanstone, *Handbook of applied cryptography*: CRC, 1997.
- [13] D. Beach, R. Mayo, R. Runkle, and D. Stephens, "Special Nuclear Materials Movement Detection Program, Radiation Sensors and Sources Roadmap," NA22-OPD-01-2010, National Nuclear Security Administration, Office of Nonproliferation and Verification Research and Development (NA-22), 2009.
- [14] R. Runkle, T. White, E. Miller, J. Caggiano, and B. Collins, "Photon and neutron interrogation techniques for chemical explosives detection in air cargo: A critical review," *Nuclear Instruments and Methods in Physics Research Section A: Accelerators, Spectrometers, Detectors and Associated Equipment*, vol. 603, no. 3, pp. 510-528, 2009.
- [15] J. Ryan, U. Bravar, E. Flückiger, J. Macri, M. McConnell, B. Pirard *et al.*, "Development and performance of the Fast Neutron Imaging Telescope for SNM detection," *SPIE: Optics and Photonics in Global Homeland Security IV*, p. 694509, 2008.
- [16] N. Mascarenhas, J. Brennan, K. Krenz, P. Marleau, and S. Mrowka, "Results with the neutron scatter camera," *IEEE Transactions on Nuclear Science*, vol. 56, no. 3, pp. 1269-1273, 2009.
- [17] E. E. Fenimore, S. D. Miller, M. M. Conrady, and J. M. Benz, "Coded-aperture imaging with uniformly redundant arrays," *Applied Optics*, vol. 17, no. 3, pp. 337-347, 1978.
- [18] M. Johnson, and M. Drigert, *COSL dosimetry for application to on-site inspections: A technical review*, LA-12619-MS UC-700, Los Alamos National Lab., NM (United States), 1993.
- [19] J. E. Tanner, S. D. Miller, M. M. Conrady, and J. M. Benz, "Autoradiography Using OSL for Monitoring Warhead Dismantlement," PNNL-SA-73268, Pacific Northwest National Laboratory (PNNL), Richland, WA (US), 2010.
- [20] J. F. Morgan, G. Ignatyev, D. Semenov, and M. Chernov, "Gamma-ray camera for arms control applications," in SPIE Society of Photo-Optical Instrumentation Engineers Annual Meeting, Denver, CO, USA, 1999, pp. 24-30.
- [21] P. Vanier, L. Forman, and D. Norman, "Thermal neutron imaging in an active interrogation environment," *20th International AIP Conference*, pp. 583-586, 2009.
- [22] M. Blackston, and P. Hausladen, "Passive and Active Fast-Neutron Imaging in Support of Advanced Fuel Cycle Initiative Safeguards Campaign," ORNL/TM-2009/210, Oak Ridge National Laboratory (ORNL), 2010.
- [23] M. Burks, J. Verbeke, A. Dougan, T. Wang, and D. Decman, "Compton DIV: Using a Compton-Based Gamma-Ray Imager for Design Information Verification of Uranium Enrichment Plants," LLNL-PROC-414476, Lawrence Livermore National Laboratory (LLNL), Livermore, CA, 2009.
- [24] A. Zoglauer, M. Galloway, M. Amman, S. E. Boggs, J. S. Lee, P. N. Luke *et al.*, "First results of the High Efficiency Multi-mode Imager (HEMI)," *2009 Nuclear Science Symposium*, pp. 887-891, 2009.
- [25] A. Heller, "A CAT Scanner for Nuclear Weapon Components," *Science & Technology Review*, <https://str.llnl.gov/JulAug09/allen.html>, 2009].
- [26] M.-A. Descalle, K. Vetter, A. Hansen, J. Daniel, and S. G. Prussin, "Detector design for high-resolution MeV photon imaging of cargo containers using spectral information," *Nuclear Instruments and Methods in Physics Research Section A: Accelerators, Spectrometers, Detectors and Associated Equipment*, vol. 624, no. 3, pp. 635-640, 2010.
- [27] E. Rhodes, and C. W. Peters, "Associated-particle sealed-tube neutron generators and hodoscopes for NDA applications," ANL/CP-74572, Argonne National Laboratory, 1991.
- [28] P. Hausladen, P. Bingham, J. Neal, J. Mullens, and J. Mihalcz, "Portable fast-neutron radiography with the nuclear materials identification system for fissile material transfers," *Nuclear Instruments and Methods in Physics Research Section B: Beam Interactions with Materials and Atoms*, vol. 261, no. 1-2, pp. 387-390, 2007.
- [29] P. Hausladen, J. Neal, and J. Mihalcz, "An alpha particle detector for a portable neutron generator for the Nuclear Materials Identification System (NMIS)," *Nuclear Instruments and Methods in Physics Research Section B: Beam Interactions with Materials and Atoms*, vol. 241, no. 1-4, pp. 835-838, 2005.
- [30] J. Mullens, J. Neal, P. Hausladen, S. Pozzi, and J. Mihalcz, "Fast coincidence counting with active inspection systems," *Nuclear Instruments and Methods in Physics Research Section B: Beam Interactions with Materials and Atoms*, vol. 241, no. 1-4, pp. 804-809, 2005.

- [31] J. Mihalcz, *Oak Ridge Multiple Attribute System (ORMAS) for Pu, HEU, HE, Chemical Agents, and Drugs*, ORNL/TM-2001/175, ORNL Oak Ridge National Laboratory (US), 2001.
- [32] G. V. Walford, J. S. Bogard, J. E. Gunning, A. M. Krichinsky, L. A. Lewis, S. E. Smith *et al.*, "Enhancing Nuclear Non Proliferation Monitoring By Overlaying Nuclear, Infrared Hyper Spectral FTIR Imaging and Optical Imaging/Scanning Detection Technologies," in *Proceedings of the Institute of Nuclear Materials Management Annual Meeting*, Baltimore, MD, 2010.
- [33] N. Bowden, M. Heffner, G. Carosi, D. Carter, P. O'Malley, J. Mintz *et al.*, "Directional fast neutron detection using a time projection chamber," *Nuclear Instruments and Methods in Physics Research Section A: Accelerators, Spectrometers, Detectors and Associated Equipment*, 2010.
- [34] C. Dickerman, E. Rhodes, G. Stanford, and A. De Volpi, "Developments in radiation hodoscope technology for arms control treaty verification," CONF-900563-7, Argonne National Lab., IL (USA), 1990.
- [35] E. Rhodes, C. Dickerman, A. DeVolpi, and C. Peters, "APSTNG: radiation interrogation for verification of chemical and nuclear weapons," *Nuclear Science, IEEE Transactions on*, vol. 39, no. 4, pp. 1041-1045, 1992.
- [36] V. Moulin, V. Rebuffel, M. Antonakios, R. Sauze, and J. Gorius, "X-ray imaging modalities for nuclear waste drums inspection," *Proceedings of the 16th World Conference on Non-Destructive Testing*, 2004.
- [37] D. Camp, H. Martz, G. Roberson, D. Decman, and R. Bernardi, "Nondestructive waste-drum assay for transuranic content by gamma-ray active and passive computed tomography," *Nuclear Instruments and Methods in Physics Research Section A: Accelerators, Spectrometers, Detectors and Associated Equipment*, vol. 495, no. 1, pp. 69-83, 2002.
- [38] D. Mercer, S. Betts, T. Prettyman, and C. Rael, "Tomographic gamma scanning of uranium-contaminated waste at Rocky Flats," LA-UR-07-5150, Los Alamos National Lab., NM (United States), 1998.
- [39] B. Sowerby, N. Cutmore, Y. Liu, H. Peng, J. Tickner, Y. Xie *et al.*, "Recent Developments in Fast Neutron Radiography for the Interrogation of Air Cargo Containers," *IAEA Conference*, pp. 4-8, 2009.
- [40] A. C. Raffo-Caiado, K. P. Zioc, J. Hayward, S. Smith, J. Bogard, and C. B. Boehnen, "Combining Measurements with Three-Dimensional Laser Scanning System and Coded-Aperture Gamma-Ray Imaging Systems for International Safeguards Applications," *Proceedings of the Institute of Nuclear Materials Management Annual Meeting*, pp. 11-15, 2010.
- [41] N. G. Cutmore, L. Yi, and J. R. Tickner, "Development and commercialization of a fast-neutron/x-ray Cargo Scanner," *Technologies for Homeland Security (HST), 2010 IEEE International Conference on*, pp. 330-336, 2010.
- [42] J. S. Hansen, "Tomographic Gamma-Ray Scanning of Uranium and Plutonium," *PANDA 2007 Addendum*, 4, 2007.
- [43] R. Estep, T. Prettyman, and G. Sheppard, "Tomographic gamma scanning to assay heterogeneous radioactive waste," *Nuclear science and engineering*, vol. 118, no. 3, pp. 145-152, 1994.
- [44] R. Venkataraman, M. Villani, S. Croft, P. McClay, R. McElroy, S. Kane *et al.*, "An integrated Tomographic Gamma Scanning system for non-destructive assay of radioactive waste," *Nuclear Instruments and Methods in Physics Research Section A: Accelerators, Spectrometers, Detectors and Associated Equipment*, vol. 579, no. 1, pp. 375-379, 2007.
- [45] R. T. Kouzes, and B. D. Geelhood, "Methods for attribute measurement and alternatives to multiplicity counting," PNNL-13250, Pacific Northwest National Laboratory, 2000.
- [46] A. Bernstein, B. Brunett, N. Hilton, J. C. Lund, and J. Van Seyoc, "The Radiation Continuity Checker: an instrument for monitoring nuclear disarmament treaty compliance," *IEEE Transactions on Nuclear Science*, vol. 49, no. 3, pp. 864-869, 2002.
- [47] L. Bond, "Inspection of Solid Rocket Motors and Munitions Using Ultrasonics," *50th JANNAF Propulsion Meeting*, 2001.
- [48] R. Hockey, "Electromagnetic Coil Technique for Arms Control Applications," in *Proceedings of the Institute of Nuclear Materials Management Annual Meeting*, Indian Wells, CA, 2001.
- [49] R. Kouzes, and B. Geelhood, "Composite Signatures of Nuclear and Non-Nuclear Technologies for Weapons Material and Component Measurement," PNNL-13861, Pacific Northwest National Lab., Richland, WA (US), 2002.

## **Appendix B: Image-Based Verification Algorithms for Arms Control (PNNL-SA-80768)**

## Image-Based Verification Algorithms for Arms Control

Sean Robinson, Ken Jarman, Allen Seifert, Ben McDonald, Alex Misner, Tim White,  
Erin Miller, and William Karl Pitts

Pacific Northwest National Laboratory  
Richland, WA  
June 9, 2011

### Abstract

Advances in radiographic material discrimination and emissive object detection algorithms are presented. This paper describes the application and challenges of improvements to material/density estimation for radiographic imaging, and outlines some of the additional algorithm work that is needed. Pacific Northwest National Laboratory is developing and evaluating radiographic image analysis techniques (active/transmission and passive/emission) for verifying sensitive objects in a material control or warhead counting regime in which sensitive information may be acquired and processed behind an information barrier. Since sensitive image information cannot be present outside the information barrier, these techniques are necessary to extract features from the full images and reduce them to relevant parameters (attributes) of the inspected items. This evaluation can be done behind the information barrier, allowing for “outside the barrier” reporting and storage of non-sensitive attributes only. Advances pertinent to an arms control context have been made to radiographic object verification algorithms, in the areas of spectral imaging for passive detectors and estimation of material density in transmission radiography images. Approaches that leverage the spectroscopic potential of the detectors are expected to allow a much greater discrimination of SNM from background and other sources. Spectral passive imaging approaches to warhead discrimination and counting include specific materials and geometric arrangement localization, as well as “spectral difference” metrics which group regions with similar spectra together. These approaches may improve resolution for discrimination between materials in addition to locating SNM within surrounding shielding and/or structural elements. Previous work by our group has developed the capability to discern material density and composition in radiographic images by examining the edge transition characteristics of objects. The material construction of an object can be investigated in this way. In a weapons counting or discrimination context, unknown occultation of objects of interest, as well as additional elements of warhead construction, construction materials of varying geometry and makeup and various angles of radiograph are expected to impact algorithm performance. Advances in material discrimination algorithms are presented as a mechanism to help make these approaches robust to these sorts of variations.

### **Introduction**

Modern imaging technology provides a wealth of information that could be used for confident verification of warheads and dismantled warhead components, if that information could be sufficiently protected behind information barriers. A companion paper explores a range of imaging systems and their potential utility in a verification setting [1]. One approach to protecting sensitive information is to reduce such image information to non-sensitive attributes that may still be used to discriminate between different material components. This kind of information about also be used to determine whether quantities of certain materials are within appropriate bounds.

To this end, earlier work by the authors included material discrimination approaches based on fitting effective geometry and attenuation parameters to images generated for a known geometric shape, with initial application to dismantlement verification [2]. This fitting method can be used to calculate density estimates for the attenuating materials within a given image region. Conceptually, this approach enables discrimination between different materials on the basis of estimated effective attenuation or density parameters. Several difficulties arise when applying this approach to more complex images, especially the presence of additional attenuators, structures or shielding components not accounted for in simplistic models.

Those previous efforts [2] hinged on the simplifying assumption that a full image (in principle using either transmission or emission radiography) would exhibit good separation between objects and thereby allow for image verification techniques based on that separation. This separation is unlikely in realistic images, due to the unknown and potentially confounding structural elements expected in real objects of interest. However, an imaging system capable of producing images as a function of energy as well as position would have the additional capability of discrimination between regions of interest by using those spectral differences.

Several improvements to the previously described material discrimination algorithm [2] can be realized by using spectroscopic information. Accurately estimating the presence of multiple materials in a single pixel requires more information than the single overall gross-count pixel intensity value. If intensity can be obtained as a function of energy by the use of an energy-sensitive imaging detector or by using several different energy spectra to provide multiple transmission radiography images, the results will supply another dimension that could be exploited. Both concepts lead to material basis function approaches that have been applied to medical imaging and explosives detection [3]. In principle, the areal densities of distinct materials can be estimated as coefficients of material basis functions through a simple attenuation equation. A benefit of this approach is that it does not depend on knowledge of geometric shape of imaged objects, allowing for a determination of the presence of materials of interest regardless of location or shape. However, to our knowledge this approach has not been previously attempted for materials with high  $Z$  (atomic number) values or with a spectroscopic imaging detector.

This paper describes the application and challenges of improvements to material/density estimation for radiographic imaging, and outlines some of the additional algorithm work

that is needed. For the analysis that follows in this paper we focus on material discrimination in simulated example transmission radiography images of an AT-400R fissile material storage container. Figure 1 shows an example simulated image in which Pu spheres are present in holders. In this figure, the darker regions indicate lower integrated flux due to greater attenuation. Images were simulated based on a 450 kVp Bremsstrahlung source that was readily available for experimental images. Analysis indicates that higher-energy sources will eventually be necessary to achieve significant penetration of the dense materials that are of interest. Nevertheless the simulated images here provide a reasonable starting point for studying the utility of material discrimination methods.

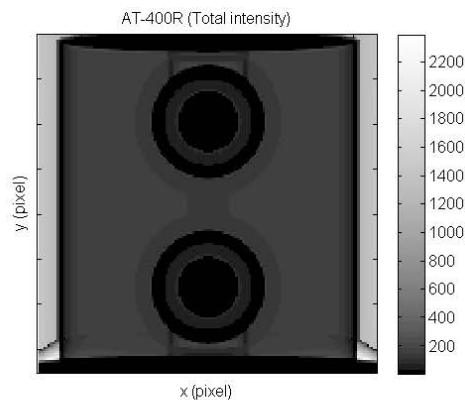


Figure 1. Simulated transmission image of AT-400R storage container. Units are gamma-ray counts summed over all energies.

### Direct Spectral Imaging

Spectral imaging (i.e. images with both spatial and energy information) can provide stronger quantification of emitting and/or highly attenuating material than non-spectral imaging. Spectral algorithms are likely most useful with passive images, in which the differences between background and sources of interest are pronounced. In passive images, regions could be evaluated with the same sorts of spectroscopic detection and identification algorithms that are used with non-imaging detectors, in this case to isolate areas of special nuclear material [4-7]. Similar algorithms may be used to enhance contrast in transmission images, and a simple illustration of this idea is given here to motivate further study. Simulated images of the AT-400R container were generated using the 450 kVp Bremsstrahlung source, and over three relatively broad energy bins: from 0 to 100 keV, from 100 to 200 keV, and from 200 to 400 keV, using the MCNP code package [8]. A simple “energy-window” ratio scheme, in which the ratio high-energy bin to the sum over all energy bins for each image pixel is calculated, demonstrates a higher perceptual contrast between dissimilar materials. Figure 2 shows the total noise-free count image, an image produced by counts in the high energy bin, and the image produced by taking the ratio of the two. Each set of image data is normalized

to a maximum value of 1 and then shown on a log scale, so that a common gray scale may be used to indicate the change in contrast.

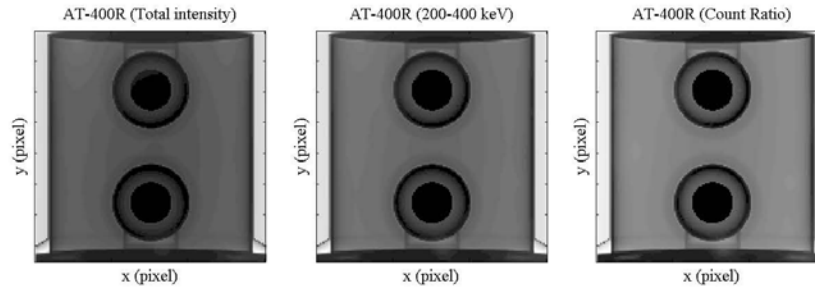


Figure 2. Image contrast enhancement using energy window ratio. Noise-free data in each image are normalized to a maximum value of 1 and log-transformed. From left to right: Total (gross count) transmission image of AT400R, high-energy (200-400 keV) counts component, and manipulated image (ratio of counts in high bin to total counts in each pixel).

It is expected that the application of this type of approach to transmission radiographs could enhance the capability of material discrimination. However, the primary utility of manipulations of this sort is expected to be found in isolating sources of interest in emission images.

**Material Discrimination Approaches**

One method used to determine the presence of materials within a transmission image is to consider a forward radiation transport model including a source, detector and an unknown catalog of intervening materials (the geometry and radiation transport of which is here modeled with MCNP [8]), and to fit the observed spectrum in each pixel to the expected data given those materials.

Here, we assume a detector that can discriminate by energy  $E$ , giving a count spectrum  $C(E)$  in each pixel that corresponds to a line from the source through the object along which we calculate the photon attenuation. We consider a set of materials, denoted by the subscript  $i$ . For the purpose of spanning likely materials and effective  $Z$  values, we have chosen the materials Polyethylene, Iron, Aluminum, and Plutonium. Our forward model for the count spectrum in a given pixel is given by

$$C(E) = S(E)D(E) \exp \left[ - \sum_i \mu_i(E) \rho_i \right],$$

where  $S$  is the source emission term (often a Bremsstrahlung spectrum in real application, so here modeled as a 450 kVp Bremsstrahlung source),  $D$  is a detector response function, the  $\mu$  terms are the mass attenuation coefficients for each material ( $\text{cm}^2/\text{g}$ ), and the  $\rho$  terms represent the areal density ( $\text{g}/\text{cm}^2$ ) of each material between the source and pixel. Counts are accumulated in  $N$  energy bins, with bin  $j$  defined by  $[E_{j1}, E_{j2}]$  and bin center  $\bar{E}_j$ :

$$C(\bar{E}_j) = \int_{\bar{E}_{j1}}^{\bar{E}_{j2}} S(E)D(E) \exp\left[-\sum_i \mu_i(E)\rho_i\right] dE.$$

The mass attenuation coefficients represent our material basis functions. This model takes into account all contributions to attenuation of a pencil beam of radiation, including attenuation due to photoelectric absorption and photons scattered out of the beam. Further approximations will be required to account for the detection of scattered radiation which may account for significant deviations from our model in images of high-density objects. Planned future study includes single-scatter approximations.

To use this model for estimating the amount of individual attenuating materials, we first need an estimate of baseline count spectra (the detector response when no attenuator is present between source and detector) and then the mass attenuation coefficients. Empirical estimates of attenuation coefficients can be obtained from existing literature or constructed from measured or simulated images. Our baseline spectra  $C_0(\bar{E}_j)$  were simulated in MCNP using the interrogating Bremsstrahlung source with no intervening materials, and mass attenuation coefficients were estimated using simulated images of uniform slabs of each material in the basis set chosen. Taking the ratio of Equation (1) for an imaged object to the baseline value produces

$$\frac{C(\bar{E}_j)}{C_0(\bar{E}_j)} = \frac{\int_{\bar{E}_{j1}}^{\bar{E}_{j2}} S(E)D(E) \exp\left[-\sum_i \mu_i(E)\rho_i\right] dE}{\int_{\bar{E}_{j1}}^{\bar{E}_{j2}} S(E)D(E) dE} \approx \exp\left[-\sum_i \mu_i(\bar{E}_j)\rho_i\right].$$

The last approximation enables relatively simple calculations for the estimation problem. For a single material, this reduces to a simple equation for  $\mu_i$  given a known density (or for  $\rho_i$  given a known mass attenuation coefficient), by which the basis functions are estimated. To generate estimates for  $\mu_i$ , uniform slabs of 3 cm were used at nominal density, and “basis images” of the form  $C_i(\bar{E}_j)$  were made for each material. For these estimates, noise-free simulations were produced, ignoring detection of scattered photons (i.e. Compton-scattered gammas were considered lost from the detector). Consequently, low-energy bins may have zero counts recorded for images of very dense slabs. The material basis functions were calculated numerically using an average of estimated values at several pixels in the center of each slab image (in this case the central  $20 \times 20$  pixel region was used). The basis functions for chosen materials are shown in Figure 3. Note the prominent Pu K-edge near 122 keV.

### Density Estimation

Given these material basis functions, areal densities of materials can be estimated from images of objects using Equation (3). There are several possible approaches to density estimation, which amounts to fitting image data to these model equations.

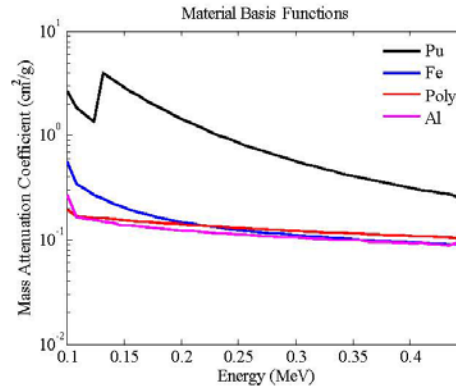


Figure 3. Basis functions  $\mu(E)$  for selected materials, units in  $\text{cm}^2/\text{g}$ .

**Estimating Density from Simulated Images – Nonlinear Optimization**

We implemented a least-squares approach to find values of  $\rho_i$  in each pixel that minimize the difference between an observed image  $C(\bar{E}_j)$  and the expected value from the forward model in Equation (1). Specifically, the log of the sum of squared errors

$$\ln \sum_j \left\{ C(\bar{E}_j) - C_0(\bar{E}_j) \exp \left[ - \sum_i \mu_i(\bar{E}_j) \rho_i \right] \right\}^2$$

was minimized using the built-in “fminsearch” function in Matlab [9]. This process was repeated for every pixel in the image, for each one fitting  $\rho_i$ , and these values were used to produce density estimates for materials in the AT-400R example. This approach requires an initial guess of material densities for each pixel, which can be found using a linear approach.

**Estimating Density from Simulated Images – Linear Regression**

With some simplifying approximations, a linear regression model may suffice for roughly estimating densities. The results may be useful in themselves or as an initial guess for the full nonlinear least squares approach. This is due to the fact that Equation (3) can be rewritten in a form that is linear with respect to the material densities:

$$\sum_i \mu_i(\bar{E}_j) \rho_i = - \ln \left( \frac{C(\bar{E}_j)}{C_0(\bar{E}_j)} \right),$$

which is linear with respect to the material densities. Given the material basis functions, the vector of areal densities  $(\rho_1, \rho_2, \dots, \rho_n)$  for  $n$  materials may be estimated using standard linear regression [10]. Note that this approach may not apply directly when there are zero-intensity pixels in several energy bins, as in the case of very dense

materials with near-zero transmission. Nevertheless it can provide initial estimates that indicate the ability to differentiate between materials before considering more complicated material basis function fitting schemes.

#### Estimating Density from Simulated Images – Nonlinear Minimization Results

Our results indicate some potential for quantitatively estimating the presence of multiple materials in simulated images of the AT-400R container. Estimation results are compared to the “true” AT-400R model here in terms of estimated total thickness of material, obtained by scaling areal density estimates by material densities. Figure 4 shows this estimated thickness at each pixel in terms of the four chosen materials Polyethylene, Iron, Aluminum, and Plutonium. Although these density “images” cannot be directly compared to transmission images shown earlier, darker pixels indicate greater total thickness of material, in a manner somewhat consistent with those earlier images. From Figure 4 we may say broadly that, except for aluminum and a pair of zero-transmission regions, the right materials were estimated in appropriate locations, and higher estimated densities for each material correspond to regions of higher actual density. Plutonium estimates are just beginning to appear at the edge of the plutonium sphere locations. However, the lack of estimates over almost the entirety of each sphere indicates an inability to quantify plutonium using the modeled Bremsstrahlung source, as the thickness of the spheres prohibited transmission flux except at the edges. It is clear that higher-energy sources are needed for this application in order to quantitatively determine the amount of very dense materials.

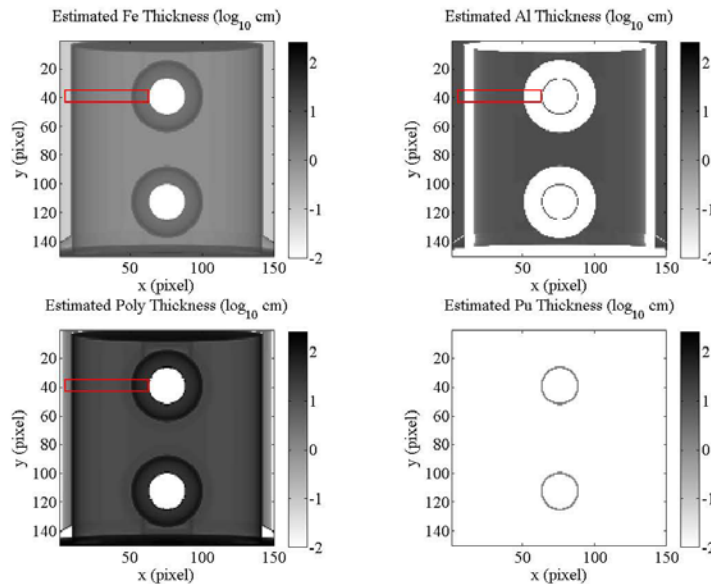


Figure 4. Estimated material thicknesses for the AT-400R image, derived from the areal density estimation scheme.

Figure 5 shows average thickness values over a portion of each “thickness image”, corresponding to a region that runs from the edge of the iron overpack can to a portion of one of the holders (indicated by a red rectangle in some of the images in Figure 4). The average is taken over the vertical within the extracted region. This figure is intended to show the transition in estimated material, from iron in the wall of the overpack can (the darker outer edge in the Fe and Poly images), to polyethylene surrounding the holder, to the holder itself, which is comprised of iron.

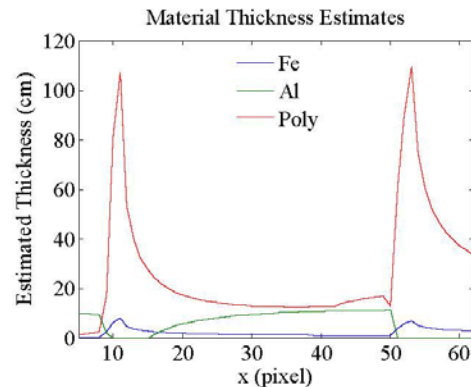


Figure 5. Estimated material thickness for the AT-400R image, derived from the areal density estimation scheme.

The figures qualitatively show the presence of the materials in the basis set within the original image. However, quantitative estimates of material do not show a great deal of fidelity. Polyethylene is over-estimated at the edge of the overpack can and at the location of the holder. The overpack can wall is approximately 0.38 cm thick, so the actual thickness of iron through two layers (e.g. in the middle of the plot in Figure 5) is around 0.76 cm; our estimate slightly exceeds this value at about 1 cm. The total amount of polyethylene in the middle of the object is around 30 cm; our estimate is under this value at approximately 13 cm. Aluminum is used only in the top and bottom of the can as part of a heatsink, but our estimate incorrectly includes several cm of aluminum. Part of the difficulty in lies in the fact that some of the basis functions are very nearly identical over much of the energy range, as can be seen in Figure 3. This similarity leads to some some misidentification of polyethylene as aluminum, as well as other “mixing” effects.

Plutonium is not included in Figure 5, as the estimated values are zero except at the edge of the plutonium spheres, where those values are poorly estimated. Notably, plutonium is only detected in the appropriate regions, and the ability to verify this fact is of potential critical importance for arms control applications. However, density estimates are not possible in this example due to the lack of flux in those regions for the particular transmission source modeled. Higher-energy sources would enable plutonium density estimation.

## Discussion

The primary goal of the material basis function approach – verifying that SNM is only estimated to be present where it actually is – appears to be accomplished in these examples. However, the reverse is not true – density estimates involving plutonium objects (in the AT-400R as well as other simulations of only Pu objects not shown here) showed a positive estimated amount of other materials, indicating that determination of the presence of other materials may not be as reliable. Additionally, the estimated materials, while qualitatively accurate in the sense of indicating greater estimated density in areas with more of that material are not particularly quantitatively accurate. This inaccuracy may be due to the high attenuation of the low-energy region, such that effectively almost no information is present in the region near the k-edges of these materials due to high scattering and absorption of gammas in these ranges. In these simulations in particular, only the Pu k-edge is included in the available data set due to the lower energy cutoff of 100 keV. The result is an effectively reduced “dissimilarity” between the observed attenuation spectra of different materials. This dissimilarity owing to the k-edge is what makes these methods effective in medical imaging. In thick regions of an object (for example, the densest paths through the AT-400R) little information in the region of the material k-edges are expected to be present due to attenuation. In real application to highly dense and high-Z objects, gamma-rays of this region will also be highly down-scattered, allowing only the higher-energy regions to contain substantial information.

To try to address this problem, one could determine how much (in terms of areal density or other property) of each of a known set of materials is present at a given pixel of an image by the use of differential methods. Under a simple assumption that the object seen in two neighboring pixels differs by at most a single material, the estimates of effective (assumed single) material properties in the two pixels should enable an estimate of the effective properties of the two individual materials in each pixel. Additionally, future application of these concepts may focus on an “effective Z” metric as estimated from the slope of the entire attenuation spectrum, rather than a linear combination of attenuation spectra from a whole catalog of materials. This approach would account for the similarity between effective  $\mu_i$  functions for each material (as the k-edges may not be observable due to high attenuation of gamma rays in that energy region) by allowing a single “shape” parameter to account for the structure of each  $\mu_i$ , and to compare these shape parameters to the observed spectrum in a single pixel of estimate an “effective Z” for that pixel.

Several factors have yet to be considered in the use of spectral methods as discussed here. Chief among these are the effects of noise and detecting scattered radiation, which must be studied to begin to make these methods practical. In particular, with dense or thick materials, Compton scattering is expected to produce a substantial number of lower-energy photons which may escape the interrogated object and be detected.

### Conclusions

Both spectral methods for contrast improvement and spectral methods for material discrimination may enhance previous attempts to discern materials within transmission and emission radiography images [2]. The results from material discrimination

approaches can be directly interrogated for the presence of nuclear materials, allowing for a simple “yes/no” metric for SNM detection to be developed. With further study to address challenges noted above, these methods may prove useful for the verification of objects in both warhead counting and dismantlement verification settings.

#### **Acknowledgements**

This research is supported by the U.S. Department of Energy National Nuclear Security Administration Office of Nonproliferation and Verification Research and Development. The Pacific Northwest National Laboratory is operated by Battelle for the U.S. Department of Energy.

#### **References**

- [1] McDonald, B.S., Seifert, A., Jarman, K.D., Robinson, S.M., Misner, A.C., Miller, E.A., White, T.A., and Pitts, W.K., Image-based verification: Some advantages, challenges, and algorithm-driven requirements (to be presented at the INMM 2011 Annual Meeting, Palm Desert, CA).
- [2] Robinson, S.M., Jarman, K.D., Pitts, W.K., Seifert, A., Misner, A.C., Woodring, M.L., Myjak, M.J., Imaging for dismantlement verification: Information management and analysis algorithms, submitted to Nucl. Instrum. Methods Phys. Res. A.
- [3] Alvarez, R.E. and Macovski A., Energy selective reconstructions in x-ray computed tomography, Phys. Med. Biol. 21(5):733-744, 1976.
- [4] Ely J., Kouzes R., Schweppe J., Siciliano E., Strachan D., and Weier D., The use of energy windowing to discriminate SNM from NORM in radiation portal monitors, Nucl. Instrum. Methods Phys. Res. A, 560:373-387, 2006.
- [5] Burr, T. and Hamada, M., Radio-isotope identification algorithms for NaI gamma-spectra, Algorithms 2:339-360, 2009.
- [6] Estep, R.J., McCluskey, C.W. and Sapp, B.A., The multiple isotope material basis set method of isotope identification with low- and medium-resolution gamma-ray detectors, J. Radioanal. Nucl. Chem., 276(3):737-741, 2008.
- [7] Hamed M.A., Gray P.W., Naboulsi A.H., MacMahon T.D., Analytical peak fitting for gamma-ray spectrum analysis with Ge detectors, Nucl. Instrum. Methods Phys. Res. A, 334(2-3):543-550, 1993.
- [8] MCNP X-5 Monte Carlo Team, MCNP—A General Purpose Monte Carlo N-Particle Transport Code, Version 5, LA UR 03 1987, Los Alamos National Laboratory, Apr. 2003. The MCNP5 code can be obtained from the Radiation Safety Information Computational Center (RSICC), P. O. Box 2008. Oak Ridge, TN, 37831-6362.
- [9] MATLAB, version 7.8.0, Natick, MA, The Mathworks, Inc. (2009).

## **Appendix C: Non-Invertible Transforms for Image-Based Verification (PNNL-SA-80555)**

## **Non-Invertible Transforms for Image-Based Verification**

**Ken Jarman, Sean Robinson, Allen Seifert, Ben McDonald, Alex Misner, Tim White, Erin Miller, and William Karl Pitts**

**Pacific Northwest National Laboratory  
Richland, WA  
June 9, 2011**

### **Abstract**

Imaging may play a unique role in verifying the presence and distribution of warhead components in warhead counting and dismantlement settings where image information content can distinguish among shapes, forms, and material composition of items. However, a major issue with imaging is the high level of intrusiveness, and in particular, the possible need to store sensitive comparison images in the inspection system behind an information barrier (IB). Reducing images via transformations or feature extraction can produce image features (attributes) for verification, but with enough prior information about structure the reduced information itself may be sufficient to deduce sensitive details of the original image. Further reducing resolution of the transformed image information is an option, but too much reduction destroys the quality of the attribute. We study the possibility of a one-way transform that allows storage of non-sensitive reference information and analysis to enable comparison of transformed images within IB constraints. In particular, we consider the degree to which images can be reconstructed from image intensity histograms depending on the number of pixel intensity bins and the degree of frequency data quantization, as well as assumed knowledge of configuration of objects in the images. We also explore the concept of a “perceptual hash” as a class of transforms that may enable verification with provable non-invertibility, leading to an effective one-way transform that preserves the nature of the image feature data without revealing sufficient information to reconstruct the original image.

### **Introduction**

Modern imaging technology provides an unprecedented capability for quantifying detailed properties of imaged objects. Existing imaging systems and recent advances such as those surveyed in the companion paper by McDonald et al. [1] could play a unique role in inspection scenarios for verifying the presence and distribution of warheads and their components. This could conceivably take the form of comparison to reference images (templates) or reduction to features similar in concept to attributes generated with non-imaging technology in current inspection scenarios. However, maintaining a

reference image requires storing sensitive information in non-volatile memory, which presents a challenge for maintaining information barrier (IB) design principles [2-6]. Moreover, imaging continues to be highly intrusive and difficult to implement with IBs. Pitts et al. [7] discuss the potential and challenge of sensitive information management with imaging systems.

To enable the use of imaging for verification, then, imaging system design and image analysis methods must be developed to address sensitive information management. Those methods must provide robust component identification and reduce the need to store sensitive reference images or sensitive image parameters, and be shown to integrate well with IB principles and practice. This paper focuses on image analysis for this purpose, as exemplified by the use of statistical methods to verify a limit on number of warheads per delivery system [8]. The Pacific Northwest National Laboratory (PNNL) has been examining analysis approaches ranging from a comparison of active (transmission) and passive (emission) images to the development of “low-intrusion” methods that do not require or report sensitive image information. Methods based on extracting physical features from radiographic images are studied in a companion paper [9]. An example discussed here is a histogram comparison technology introduced earlier, in which pixel intensities are binned to establish non-sensitive image feature vectors that cannot in general be inverted to uniquely return the image [10]. This technique thus resembles a one-way hash function for images and could be expected to be acceptable in inspection scenarios. The utility and importance of such one-way transforms in the context of maintaining a verifiable count of nuclear weapons systems was recently emphasized by Fuller [4].

An image processing approach known as “perceptual hashing” may add a robust layer of security to features extracted via any of the methods highlighted above. The approach is drawn from image processing applications to multimedia content authentication, image tampering detection, and image database search. The underlying idea is that images that would be perceived to be the same (e.g. by a knowledgeable observer) in spite of small differences in digital representation should be declared a match by image verification methods. Reduction of images to relatively short numerical representations, such as those produced by hash functions, enables rapid search of large image databases and robust image tampering detection. However, cryptographic hashing is sensitive to a single bit change, destroying the ability to identify perceptually matching images unless they can be first reduced to identical data. So-called perceptual hashing represents a combination of image processing techniques and hashing for matching perceptually identical images [11-13]. This approach uses a variety of image reduction techniques to extract robust features from the image, followed by traditional hashing. These robust features must be invariant to small variations to the image, such as noise, scaling, or rotations, as would be expected from repeated radiographic inspection of an identical object. Thus in principle the concept applies directly to features derived from images in an arms control context as well.

In this paper we discuss the balances between true and false identification, and between protecting sensitive information and verifying imaged objects using an image histogram

technique. In particular, we discuss the potential for using a perceptual hash as a provable one-way transform for robust and secure verification.

**Histogram Comparison**

We first discuss an image data reduction technique that may enable verification while inherently protecting sensitive information, possibly allowing the reduced image to be viewable outside an IB. The intent with image histograms is to bin pixel intensities to establish non-sensitive image feature vectors that cannot in principle be inverted to uniquely return the input image. This one-dimensional reduction of two-dimensional data could then be used as a reference to be compared to an image histogram of an inspected object. Figure 1 shows a schematic of the verification process concept based on histograms.

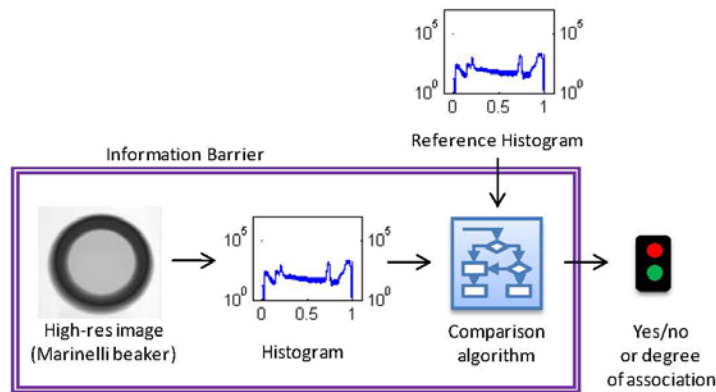


Figure 1. Conceptual use of histogram comparison with information barrier for object verification.

Robinson et al. [10] studied this concept using transmission images of beakers containing material of different densities. Results indicated confirmation of objects with the same density and structure and discrimination between objects with different densities or structures. In those examples the variation between images in terms of object orientation and spatial arrangement of transmission source, imaged object, and detector was tightly controlled. The degree of variation expected in realistic inspection scenarios would need to be well characterized to apply this approach.

Some amount of structure within the images will be represented in the histograms. Very similar histograms can potentially confirm detailed image structure without the reference histogram giving away sufficient detail to reconstruct the image. However, verification requires an expectation that at least some general structure is consistent in the two images (e.g. general arrangement of warhead components). If enough detail of that structure and the reference histogram were to be known outside an IB *a priori*, they could be used to

constrain the population of possible images that produce the reference histogram, and thus present a risk of discovery of the original sensitive image from the reference.

A simple example may illustrate this part of the challenge in managing sensitive information with a histogram approach. The 5-by-4-pixel two-level binary images in Figure 2 produce the same binary histogram, (6,14) (i.e. 6 pixels in each image are white while 14 are black). Several other arrangements produce the same histogram as well; the structure and features in the histogram cannot be used to uniquely reconstruct the source image. Suppose the reference object can only be formed in an S-shape and that this information is sensitive and is known only to a “host”. Knowing the reference histogram in this case does not reveal the sensitive information to an “inspector”. However, the inspector may have enough knowledge of expected structure or other features to eliminate many cases from consideration. For example, suppose the inspector knows that the structure primarily consists of a contiguous, “single-block-wide” shape. A subset of images including the first two in Figure 2 would also meet this criterion, but certain reconstruction of the image is still not possible. Nevertheless, to the degree that the set of images that meets such known criteria can be reduced, the risk of successful “attack” on the reference histogram, and the resulting sensitive information release, increases.

In this example, a positive match between a histogram of the inspected object and the reference histogram is considered a true verification. A second issue that arises is the possibility of spoofing the inspection. The host may be able to modify an inspected object to be in any other arrangement that produces the same histogram. For the purpose of this example it may be assumed that either no such modification is possible or it could be indicated by other means of inspection.



Figure 2. Similar structures in three different 5-by-4-pixel images.

Realistic images and structure are much more complex than the simple example given here for illustration. With this additional complexity, it is likely that reconstructing the original image from a histogram with any degree of confidence becomes much more difficult. Additional study is needed to address the degree to which reconstruction is possible. If reconstruction is not possible, then this technique resembles a one-way hash function for images. The potential for spoofing the comparison via modified object structure must also be studied. Very dissimilar objects could produce the same histogram as the reference object and could therefore be used to spoof histogram comparison. Solutions to the problem of spoofing may include the use of additional one-way image reductions or other means to indicate possible modification. Other interrogation methods could detect such modifications, and it is likely that a combination of methods would be used for verification.

Two key issues arise in the above discussion that can be characterized in terms of feature “resolution” parameters. For example, fewer bins and count levels (e.g. low/medium/high vs. integer counts in each bin) make for more coarse histograms. As fewer bins and levels are used, images with greater variation (e.g. noise) become more likely to be declared a match. This leads to both higher true and false “verification”, and the balance between the two as a function of histogram resolution must be studied.

Second, the degree of success of an “attack” on a reference histogram attempting to reveal sensitive information also depends on the histogram parameters. At the same time, confident verification requires a relatively high level of detail. Thus a challenge with this approach is to determine the level of reduction, in terms of the two histogram parameters (number of bins and frequency levels reported) that balances between the demands of verification (high true verification and low false “verification”) and protecting sensitive information. This challenge is currently under study.

The “perceptual hash” described in the next section may solve the problems of both spoofing and attacks attempting to reveal sensitive information, by moving image comparison to the level of a cryptographic hash rather than a histogram (for example). That approach provides a layer of proven one-way transformation that may address these fundamental issues.

The “one-way transform” discussion above suggests the potential for comparison to a reference outside of an information barrier. IBs, consisting of a collection of physical obstructions, instrument firewalls, volatile data storage, rigorous procedural control, and other techniques, are designed precisely to strike the balance between protecting sensitive data and disclosing sufficient information to establish that the item in question is as declared (verification) [2-6]. Generating image data and an associated histogram could be performed in volatile memory, and only the histogram itself would be provided for comparison to the non-sensitive reference histogram.

### **Perceptual Hash**

On its own, a histogram or other image reduction may ultimately present too great a sensitivity risk to be used outside an IB, and a further level of protection may be needed. True hash functions, which are provably one-way transforms of messages into condensed output messages, could provide this additional protection [14]. Hashes are already implemented in IBs to ensure authentication of the system memory and loaded software by reducing an input string and total system memory storage to a defined hash output. This component of the authentication process assesses confidence in the overall system performance, including security considerations [15]. It could conceivably also be used in a similar manner to securely pass the information contained in images for verification.

The main problem with this concept for image-based comparison is that hash function output is sensitive to even a single-bit change. Considering the variety of sources of variation in images in a verification setting (e.g. noise, orientation and other geometric

distortions), it cannot be expected that a given image of an inspected object, or a histogram of that image, would exactly match that of a reference object. What is needed is a method that can confidently verify a match between two images that would be perceived to be identical but for insignificant variations, while maintaining as much as possible the benefits of a hash function.

An approach developed for multimedia content authentication, image tampering detection, and image database search may provide such a method. The so-called “perceptual hash” combines image reduction techniques, like the histogram, with hash functions to provide compact representations of images for comparison [11-13]. Images in this context often undergo slight transformations due to compression, geometric distortion (e.g. affine transformations), filtering, enhancement, or noise corruption. The key element is the representation of reduced images (e.g. features) on a coarse enough level that exact matches can be made between images that would be perceived to be the same in spite of small variations.

Figure 3 shows a schematic of the process as envisioned here, which could take two paths within the IB. Internally, an image is processed into a reduced, coarsened set of information that is robust to small variations, prior to hashing. This could take place by first applying a transformation (e.g. histogram or feature extraction) and then representing that information at a coarse level (e.g. coarse bin structure and frequency levels in histograms), or by first coarsening the original image and then transforming the coarse image. This process is well-suited to the histogram comparison approach in which the coarsening of information is proposed as part of the mechanism for balancing verification demands.

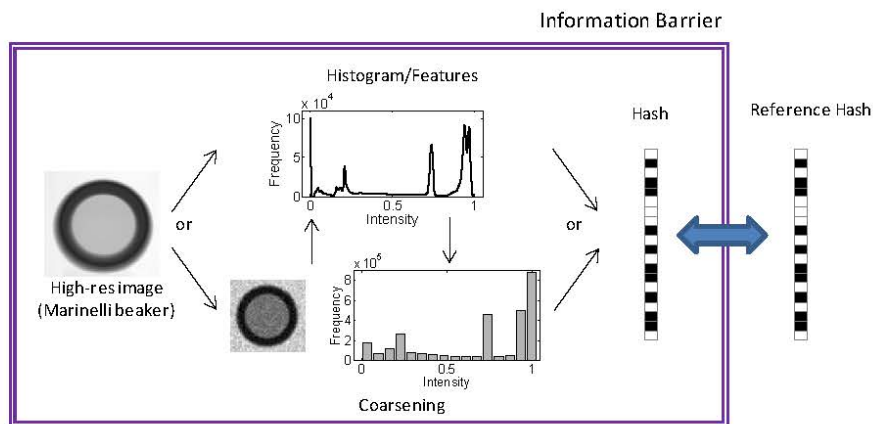


Figure 3. Conceptual use of histogram comparison and hashing to compare to a non-sensitive reference hash outside an information barrier for object verification.

The perceptual hash achieves a level of robustness against mild variation through the data reduction/coarsening step. For example, histograms with a large number of bins and frequency levels for two independent noisy images of the same object will not match exactly. At some level (dependent on the magnitude of noise), coarser histograms will match. A variety of techniques for image reduction are evident in the perceptual hash literature, including various transformations, feature extraction, image coarsening, and calculation of image statistics. Examples include coarsening images to very few pixels (e.g. block-averaging) followed by thresholding against local averages or medians to create a binary image (which is then hashed) [16]; wavelet filtering to compute mean low-frequency and variance of medium- and high-frequency information [17]; and a histogram method similar to that described here [18]. Results from these and several other efforts indicate that perceptual image hashing is an effective approach for matching and detecting modifications of images in the presence of limited variation.

Because the histogram comparison technique can be incorporated into the perceptual hash concept, the challenges raised for the former may be best addressed within this context. A first challenge relates to protecting sensitive information. If enough details of the perceptual hash are known to both parties in an inspection setting (this may include secret keys), then robustness of the process to slight variations may leave it vulnerable to attack. Specifically, a search for images that produce the same perceptual hash is conceivably much easier than searching for the one that produces a unique cryptographic hash. A second relates to spoofing. Again, if enough details are known, a host may be able to spoof the system by presenting a modified object that produces the same perceptual hash. A solution to this problem may be the use of multiple measures in verification, some of which are aimed at detecting such modification. Also as noted earlier, changing data reduction parameters impacts both the ability to verify and protect information. The tradeoff between positive and false identification of an object as a function of these parameters is currently being studied. This may include limited “red-teaming” efforts to assess confidence in the approach at a basic level.

### **Conclusions**

PNNL is studying the application of possible non-invertible (one-way) transforms for image-based verification based on image histogram comparison and perceptual hash algorithms. The perceptual hash can incorporate and enhance the histogram approach, and may incorporate any alternative methods for image reduction.

While some excellent results have been obtained for the perceptual hash in different applications, an ability to simultaneously verify declared items and protect sensitive information in inspection settings must be demonstrated in principle. The appeal of implementing a perceptual hash concept lies primarily in its reliance on well-established cryptographic hash results, and the acceptance of hashing in IB technology.

In terms of comparison to a reference, conceptually the process can be thought of in terms of comparing either the original images or a specific reduction of those images. A perceptual hash could also be applied to any attributes derived from images based on

PNNL-SA-80555

physical principles and result in a template derived from agreed-upon attributes. In any case, perceptual hashing may allow templates to be used without the need to store sensitive data. Thus the perceptual hash concept has potential broad application for enabling imaging in arms control.

### **Acknowledgements**

This research is supported by the U.S. Department of Energy National Nuclear Security Administration Office of Nonproliferation and Verification Research and Development. The Pacific Northwest National Laboratory is operated by Battelle for the U.S. Department of Energy.

### **References**

- [1] B.S. McDonald, A. Seifert, K.D. Jarman, S.M. Robinson, A.C. Misner, E.A. Miller, T.A. White, and W.K. Pitts, "Image-based verification: Some advantages, challenges, and algorithm-driven requirements" (to be presented at the INMM 2011 Annual Meeting, Palm Desert, CA).
- [2] R. Whiteson and D.W. MacArthur, "Information Barriers in the Trilateral Initiative: Conceptual description," Los Alamos National Laboratory, LAUR-98-2137 (Unlimited distribution, available from the United States Department of Energy, Office of Scientific and Technical Information website, [www.osti.gov](http://www.osti.gov)), 1998.
- [3] Technology R&D for Arms Control, Tech. Rep. NNSA/NN/ACNT-SP01, Office of Nonproliferation Research and Engineering (ONRE), U.S. Department of Energy (Spring 2001).
- [4] J.L. Fuller, "Verification on the road to zero: Issues for nuclear warhead dismantlement," Arms Control Today ([http://www.armscontrol.org/act/2010\\_12/%20Fuller](http://www.armscontrol.org/act/2010_12/%20Fuller)), December 2010.
- [5] J.K. Wolford, Jr. and G.K. White, "Progress in gamma ray measurement information barriers for nuclear material transparency monitoring," in Proc. INMM 2000 Annual Meeting, New Orleans, LA, 2000.
- [6] R.T. Kouzes and J.L. Fuller, "Authentication of monitoring systems for nonproliferation and arms control," in Proc. Symposium on International Safeguards: Verification and Nuclear Material Security, International Atomic Energy Agency, Vienna, Austria, 2001, IAEA-SM-367/17/05.
- [7] W.K. Pitts, K.D. Jarman, E.A. Miller, B.S. McDonald, A.C. Misner, M.J. Myjak, S.M. Robinson, A. Seifert, C.E. Seifert, and M.L. Woodring, "Advantages of dual mode imaging for managing sensitive imaging information," in Proc. INMM 2010 Annual Meeting, Baltimore, MD, 2010.

- [8] P.C. Schaich, G.A. Clark, S.K. Sengupta, and K.-P. Ziocck, "Automatic image analysis for detecting and quantifying gamma-ray sources in coded-aperture images," *IEEE Trans. Nucl. Sci.*, 43(4), 2419-2426, 1996.
- [9] S.M. Robinson, K.D. Jarman, A. Seifert, B.S. McDonald, A.C. Misner, Tim White, E.A. Miller, and W.K. Pitts, "Image-based verification algorithms for arms control" (to be presented at the INMM 2011 Annual Meeting, Palm Desert, CA).
- [10] S.M. Robinson, K.D. Jarman, E.A. Miller, A.C. Misner, M.J. Myjak, W.K. Pitts, A. Seifert, C.E. Seifert, and M.L. Woodring, "Image analysis algorithms for dual mode imaging systems", in *Proc. INMM 2010 Annual Meeting*, Baltimore, MD, 2010.
- [11] R. Radakrishnan, Z. Xiong, and N. Memon, "On the security of the visual hash function," *J. Electron. Imaging*, 14(1), 013011, doi:10.1117/1.1867475, 2005.
- [12] A. Swaminathan, Y. Mao, and M. Wu, "Robust and secure image hashing," *IEEE Trans. Inf. Foren. Sec.*, 1(2), 215-230, 2006.
- [13] V. Monga and B.L. Evans, "Perceptual image hashing via feature points: Performance evaluation and tradeoffs," *IEEE Trans. Image Process.*, 15(11), 3452-3465, 2006.
- [14] A. Menezes, P. van Oorschot, S. Vanstone (Editors), *Handbook of Applied Cryptography*, CRC Press, 1996.
- [15] R.R. Hansen, R.B. Bass, R.T. Kouzes, and N.D. Mileson, "Implementation of the AES as a hash function for confirming the identity of software on a computer system," PNNL Report PNNL-14170, January 2003.
- [16] B. Yang, F. Gu, and X.Niu, "Block mean value based image perceptual hashing," in *Proc. International Conference on Intelligent Information Hiding and Multimedia Signal Processing (IIH-MSP'06)*, IEEE, 167-172, 2006.
- [17] R. Venkatesan, S.-M. Koon, M.H. Jakubowski, and P. Moulin, "Robust image hashing," in *Proc. IEEE International Conference on Image Processing (ICIP'00)*, IEEE, 664-666, 2000.
- [18] S. Xiang, H.-J. Kim, and J. Huang, "Histogram-based image hashing scheme robust against geometric deformations," in *Proc. 9th workshop on Multimedia & Security (MM&Sec'07)*, ACM, 121-128, Dallas, TX, 2007.

**Appendix D: Imaging for Dismantlement Verification:  
Information Management and Analysis Algorithms [Accepted  
for publication in Nucl. Instrum. Methods Phys. Res. A.];  
(PNNL-SA-78495)**

## Imaging for dismantlement verification: information management and analysis algorithms

S.M. Robinson\*, K.D. Jarman, W.K. Pitts, A. Seifert, A.C. Misner,  
M.L. Woodring, M.J. Myjak

*Pacific Northwest National Laboratory, Richland, Washington 99352 USA*

---

### Abstract

The level of detail discernible in imaging techniques has generally excluded them from consideration as verification tools in inspection regimes. An image will almost certainly contain highly sensitive information, and storing a comparison image will almost certainly violate a cardinal principle of information barriers: that no sensitive information be stored in the system. To overcome this problem, some features of the image might be reduced to a few parameters suitable for definition as an attribute, which must be non-sensitive to be acceptable in an Information Barrier regime. However, this process must be performed with care. Features like the perimeter, area, and intensity of an object, for example, might reveal sensitive information. Any data-reduction technique must provide sufficient information to discriminate a real object from a spoofed or incorrect one, while avoiding disclosure (or storage) of any sensitive object qualities. Ultimately, algorithms are intended to provide only a yes/no response verifying the presence of features in the image. We discuss the utility of imaging for arms control applications and present three image-based verification algorithms in this context. The algorithms reduce full image information to non-sensitive feature information, in a process that is intended to enable verification while eliminating the possibility of image reconstruction. The underlying images can be highly detailed, since they are dynamically generated behind an information barrier. We consider the use of active (conventional) radiography alone and in tandem with passive (auto) radiography. We study these algorithms in terms of technical performance in image analysis and application to an information barrier scheme.

*Keywords:* arms control, information barrier, treaty verification, warhead dismantlement

---

\*Corresponding author  
Email address: sean.robinson@pnl.gov (S.M. Robinson)

## 1. Introduction

Multi-party agreements and regimes may require the joint inspection of sensitive items. Inspectors might confirm that a small number of sensitive items are in a set of storage containers by making key measurements after these containers have been sealed. These measurements form the basis of comparison for later inspections of equivalent sealed containers. Preventing disclosure of sensitive information during measurements is critical for multi-party agreements and generally required by security regulations. Hence, information barriers (IBs) used to protect sensitive information from disclosure are typically established using a collection of physical obstructions, instrument firewalls, volatile data storage, rigorous procedural control, and other techniques. The inspections must achieve a balance between protecting sensitive data (certification) and disclosing sufficient information to establish that the container holds the declared item (authentication) [1–4].

These two processes have similar actions and outcomes but each reflects the differing constraints of the host and monitor/inspector. Certification is the process used by the host's security organization to demonstrate that the host's sensitive information is protected from disclosure to the monitor. In general, it is considered to be a private inspection without monitor participation. As far as the IB is concerned, it is typically considered to mean that the IB is sufficiently robust or hardened to protect sensitive information. Authentication is strictly defined as the process by which a Monitoring Party gains appropriate confidence that the information reported by a monitoring system accurately reflects the true state of the monitored item. Unlike certification, which is expected to be a host-only process, authentication is expected to be a process directed by the monitor and performed by the host. While both processes are expected to include similar features such as physical, electronic, and cyber inspection, clearly certification can more easily be made a rigorous process. A key feature of IB design is that sensitive information is not stored in the system since rigorous authentication requires monitor access to all software and stored information.

Figure 1 gives a conceptual illustration of the overall verification process.

Radiation imaging is not normally incorporated into the verification process due to the level of sensitivity inherent in a high-resolution radiograph of an object. Assumptions that imaging is too invasive and too difficult to implement behind an IB have led to imaging being routinely dismissed as a verification technique. While imaging is invasive, its capability to assess form and function could be key to enabling future material or item control regimes. For example, imaging gives the spatial relationship between subassemblies in the object to be verified, which provides one of the strongest diagnostics in assessing the intended function of that item.

Operating an imaging analysis algorithm reliably and autonomously behind an IB presents a technical challenge. However, whether or not imaging is accepted or rejected is ultimately a policy decision, not a technical decision. The main obstacle for using imaging is that simple comparison techniques require

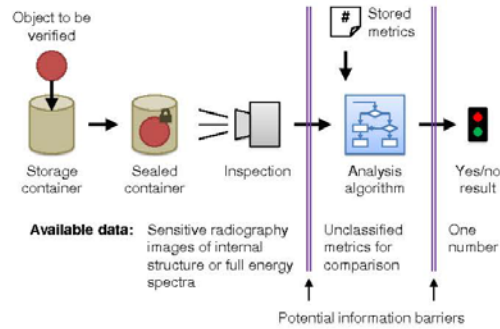


Figure 1: Conceptual illustration of dismantlement verification process.

a stored reference image or set of parameters. Storing sensitive image information violates a cardinal principle of IB design. In addition, there has been a perception that other measurements, including high-resolution gamma-ray spectroscopy and neutron counting, give adequate information for many applications, such as SNM mass attribute measurements. However, the simple attributes defined for material control may not have sufficient fidelity to distinguish treaty-limited items, such as components or assemblies, from non-limited items, such as stored sensitive material. Imaging might also have a role in a material control regime where SNM is stored in a particular declared configuration and/or chemical form. A summary of the technical challenges facing Arms Control appears in [5].

Algorithms are developed in this work which allow for discrimination of objects without the need for storage of sensitive image data. In this paper, we briefly summarize two imaging techniques, discuss the utility of imaging in the context of Arms Control, and give some considerations for information barriers. We then present three potential image analysis algorithms that do not store nor disclose sensitive information about the item of interest. Finally, we give some results that illustrate the performance of the algorithms with various objects, intended to provide an example of discrimination between objects.

## 2. Imaging Techniques

A verification system can use radiography in both active and passive modes for scanning objects. In active radiography, a strong x-ray source is placed on one side of the object, and a large-area imaging detector is placed on the opposite side. An image is then made from the transmitted photon flux. The image formed on the detector is representative of the attenuation of the x-rays through the intervening materials (including the container and contents). Radiography

techniques range from non-electronic dose-recording films to sophisticated imagers used for industrial applications. Depending upon the quality of the images and characteristics of the imaging device, the information ranges from a simple high-contrast image showing the size and shape to a detailed image that can be analyzed for attenuation along the edges. Active imaging can be useful for discriminating materials and providing densitometric information about the field of view, but does not provide information regarding radioactive isotopes present in the object.

In passive imaging, or autoradiography, the radioactive object is used as the source for an imaging system such as a coded aperture imager or Compton-imaging system. A number of techniques exist for this purpose [6, 7]. In coded aperture imaging, emissions from the target object are attenuated through a mask pattern and create a projection on a position-sensitive detector. The mask pattern is designed to render the detector response to a single point source as close to unique as possible [6, 8]. Coded aperture imaging works well with the lower-energy gamma rays from SNM due to the attenuation factor of necessarily thin mask shielding. Coded aperture imaging has found use in imaging objects which are compact in the field of view, ranging in application from gamma-ray astronomy to national security [9].

Imaging techniques could also include a subset of active radiography using an external radiation source. This source can be used to induce nuclear reactions in the material, generating a secondary radiation signature [10, 11]. The drawback of passive imaging systems for SNM measurement is that little or no information about object density is readily obtainable. Potentially, a solid mass of SNM could be replaced with a less dense object coated with a layer of SNM without significantly affecting the gamma-ray emissions from the surface. In addition, the passive radiograph generally has significantly lower resolution than does an active radiograph. For instance, the resolution of coded aperture imaging is often limited by the size of the mask holes and the tradeoff between resolution and sensitivity.

While passive radiography may be more effective at verifying the specifics of radioactive material distribution, active radiography may be more effective at verifying material density and structure. Using both active and passive imaging systems may improve the likelihood of detecting material diversion, by making it more difficult to "spooft" both systems at the same time. This report provides a general notion of how the information from the two imaging modalities may be integrated to improve verification efforts.

The radiation and passive image of a sealed container together contain a large amount of information. The active radiograph can be processed to give the overall size, geometry, edge characteristics, and density of the constituent item. These parameters are interrelated. Edge characteristics and density are generally related to each other as well as to the chemical form of the item, such as plutonium oxide or metallic plutonium. The geometry and edge characteristics should be related as well: for example, a plutonium cylinder ("hockey puck") viewed edge-on will have a significantly different edge profile between the curved sides and flat top or bottom. The passive autoradiograph generally indicates the

distribution of radioactive material within the container. One can also extract position-dependent spectroscopic information from the passive imaging system, which could be analyzed to determine whether a particular region of the image had the expected radiation signature.

### 3. Information Barriers

The IB and associated operating procedures are necessary components for an image-based verification system to protect sensitive data from disclosure during inspection. The IB usually has several components: tamper-indicating enclosures around the measurement system to prevent unauthorized access, interlocks that shut down the system immediately upon tampering, and one-way data transfers that transmit the minimum required information. A key related concept is the reduction of measurements to a particular attribute with a defined yes/no outcome [1]. Attributes are related to sensitive data but they do not themselves contain sensitive information. An exact isotopic enrichment, for example, may be sensitive, while an enrichment attribute defined as a range or threshold could be acceptable. Another example is that a nominal stored mass might be declared with a mass attribute being a yes/no mass measurement within a related mass range. Reducing a sensitive measurement to an attribute simplifies the information barrier: the data output can be a simple yes/no result implemented with a one-way display. At the same time, information into the system is restricted by reduction to an attribute, thereby closing a possible path for tampering. The input data path might only be an identified path for a test or calibration item, for example. In all cases the flow of information is reduced to a minimum.

In order for imaging algorithms to be acceptable in an IB regime, then, several requisite factors must be met. First, no original image data (and no data from which a full image could be reconstructed) may be stored in non-volatile memory since that memory is likely to be inspected by the monitor during the authentication process. Any imaging scheme must not return or store information from which size, shape of sensitive aspects of material composition could be reconstructed. Also, the information used to make the "yes/no" comparison cannot be sufficiently related to these attributes that measuring them amounts to revealing sensitive data. The algorithms presented here are studied in regard to these criteria as well as their effectiveness in discriminating objects of interest.

### 4. Analysis Algorithms

We explored several possible ways to deal with information security restrictions on the use of imaging in an Arms Control context, while maintaining the ability to distinguish between imaged objects. The first approach is to sufficiently obscure both the reference and acquired images to the point where the information can be displayed outside an IB. This process must remove the

#### 4.1 Histogram Comparison

6

possibility of inversion in a manner analogous to cryptographic hash functions. Another approach is to perform an internal analysis directly on the sensitive information behind the IB, returning a non-sensitive quantity; this alternative eliminates the need to store reference images (original or obscured) or other potentially sensitive parameters. A third approach is to compare active and passive radiographs of the same object behind the IB. This section presents three image analysis algorithms that were inspired by these respective information management strategies. We focused on two goals when developing the algorithms: the ability to distinguish between objects of different density, shape, and radioactive profiles, and the effectiveness of obscuring information more specific than the algorithms are designed to verify.

##### 4.1. Histogram Comparison

The need for sensitive discrimination between potentially similar images as well as the desirability of retaining a template from a trusted object to use as a comparison against further objects suggests that a scheme similar to cryptographic hashing be employed [12]. Cryptographic hash functions are one-way transforms that take the entirety of a large message or file and reduce it to a condensed output message. It is fundamental that the hash function output cannot be used to recreate the original message. Because the cryptographic hash function is a one-way transform, there is no method to extract the sensitive state of the stored data on the system.

For image-based verification analysis, we desired an image data reduction scheme that removes the possibility of inversion while maintaining similarity across similar images (a facet that most cryptographic hash schemes lack by design, as changing one bit of input would also change the hash output). To this end, the first algorithm works by computing a histogram of pixel intensities from an active radiography image, effectively reducing the 2D spatial image into a 1D space. To the degree that constraints such as the structure of stored dismantlement components are not sufficiently known *a priori*, this process can eliminate the possibility of explicit inversion. The issue of invertibility is discussed further below. The histogram from the interrogated object can then be compared to a previously generated “template” histogram to determine a degree of similarity with the expected object. This histogram template would be stored on the system.

To study the capability for distinguishing between objects on the basis of pixel intensity histograms, we consider a set of image histograms with two or more groups of like images. We then estimate a comparison metric for every distinct pair of images, both for the within-group populations and the across-group populations. The average separation between within-group comparisons and across-group comparisons was considered to be the “resolving power” of this method, as greater separation suggests higher discriminating power. We used a two-sample statistical hypothesis test statistic to represent the average separation. Resolving power is quantified by an approximate statistical significance level.

4.1 Histogram Comparison

7

We tested a number of histogram comparison functions. A simple dot product (evaluating the inner product between two vectors of histogram intensities) produced promising results and is the comparison function considered here. Let  $A_{ij}$  be an image for  $i = 1, \dots, M_j$  images in  $j = 1, \dots, N$  groups. Let  $X_{ij}$  be the vector representing the histogram of pixel intensities for image  $A_{ij}$ , and let  $\rho_{ijkl} = X_{ij} \cdot X_{kl}$  be the dot product. Estimates of the within-group distribution mean and variance are as follows:

$$\bar{\rho}_{jj} = \binom{M_j}{2}^{-1} \sum_i \sum_{k>i} \rho_{ijkj}, \quad s_{jj}^2 = \left[ \binom{M_j}{2} - 1 \right]^{-1} \sum_i \sum_{k>i} [\rho_{ijkj} - \bar{\rho}_{jj}]^2.$$

This definition considers all unique pairs of non-identical images. Similarly, estimates of the across-group distribution mean and variance are as follows:

$$\bar{\rho}_{jl} = (M_j M_l)^{-1} \sum_i \sum_k \rho_{ijkl}, \quad s_{jl}^2 = (M_j M_l - 1)^{-1} \sum_i \sum_k [\rho_{ijkl} - \bar{\rho}_{jl}]^2.$$

We want to know whether across-group comparisons are significantly different from within-group comparisons. One way to answer this question is to use a two-sample  $t$ -test for significant difference between the means, accounting for the difference in variances [13]. The approximate test statistic

$$\frac{|\bar{\rho}_{jl} - \bar{\rho}_{jj}|}{\sqrt{s_{jl}^2 (M_j M_l)^{-1} + s_{jj}^2 \binom{M_j}{2}^{-1}}}$$

indicates the resolving power between groups of different images. Applying the  $t$ -test then provides a threshold against which this quantity can be compared to determine whether the resolving power is significant.

The question remains whether the histogram of pixel intensities is a sufficient one-way transform to fully protect sensitive information about the original image. A given image with  $m \times n$  pixels can be rearranged in  $(m \times n)!$  ways to produce other images with exactly the same histogram. This very large number of combinations makes any direct inversion prohibitive for all reasonable image sizes. However, it may be possible to extract some information about the imaged object from the intensity histogram. The fraction of “black/very dark” and “white/very light” pixels gives a measure of the overall size of the item relative to the imager’s field of view. In addition, the fraction of “gray/transition” pixels give an overall estimate of the size of the edge. Using a lower number of pixels and a limited gray scale range limit the information that can be extracted. The limits on determining an object’s size and edge transition can be found for a given bin size in the histogram. Once that technical result is known, the next step is determining whether the histogram binning scheme inherently protects sensitive information; if so, then the histogram should be viewable through an information barrier, and a reference histogram may be stored. We plan to pursue these questions in future work.

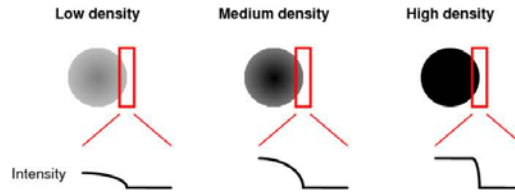


Figure 2: Determination of material density examining the intensity gradients at the edge.

4.2. Material Recognition

Given an active image of an object, some amount of *a priori* knowledge of the object’s general shape can be exploited to estimate attenuation characteristics and, ultimately, density of the material. The material recognition approach uses the pixel intensity gradients near the edges of the object to distinguish between lighter and denser materials. We developed algorithms for spherical objects as a relatively simple example. Figure 2 illustrates the overall concept behind the algorithm. The higher the material density, the sharper the transition from light to dark at the object’s edge.

In addition to knowing the shape of the object, a rough initial estimate of location and spatial dimensions is assumed. One way to obtain such an estimate is to use existing image analysis methods for locating and characterizing specific shapes within images. The Hough Transform, for example, can be used to locate circles which could indicate spherical imaged objects [14]. Our initial testing of the circular Hough transform for this purpose showed promise, but is not the focus of the present study. Using Beer’s Law and the parametrization of a sphere, we can then estimate attenuation factor by fitting that parametrization to a set of pixel intensities that correspond to some part of the sphere.

Let  $I_{ij} = I_0 \exp(-\mu d_{ij})$  be the intensity at pixel  $(i, j)$  within the sphere, where  $d_{ij}$  is the depth of the sphere at that pixel and  $\mu$  is the attenuation factor for the material. The attenuation factor can be used as a discriminator of the type of material, given assumptions about the nominal densities of possible materials. An estimate for the unattenuated pixel intensity is assumed to be obtainable by a “blank” image or portion of the object image outside the sphere. In units of pixels, a sphere with center  $(i_c, j_c)$  and radius  $R$  is defined by

$$(i - i_c)^2 + (j - j_c)^2 + (d_{ij}/2)^2 = R^2.$$

Substituting for  $d_{ij}$  in the equation for the sphere and re-arranging gives the following equation:

$$[\log(I_{ij}/I_0)]^2 = 4\mu^2 [R^2 - (i - i_c)^2 - (j - j_c)^2].$$

Given pixel intensities and an estimate of no-attenuation pixel intensity, parameters  $(i_c, j_c)$ ,  $R$ , and  $\mu$  are simultaneously estimated using nonlinear regression.

## 4.3 Active/Passive Pixel Correlation

9

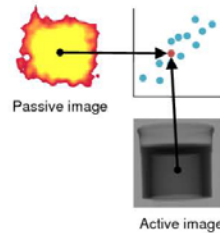


Figure 3: Schematic for comparison of active and passive images for identifying dense, emissive material.

The estimate of  $\mu$  can be compared to empirical or simulated parameter values for a variety of materials to help verify the presence of a particular material.

Like the histogram comparison algorithm, the material recognition technique is designed not to disclose sensitive information. Although the radius of the object is computed as part of the process, only the material attenuation factor needs to be reported. The technique would be especially useful to distinguish between chemical forms since the metallic and oxide forms have very different densities. Hence, the output might be well suited to a metal/oxide attribute.

## 4.3. Active/Passive Pixel Correlation

The third algorithm studies the correlation between pixel intensities in the active and passive images of the same object in the same orientation. The key idea behind this algorithm is that the dense items in the container will be the most radioactive, whereas the surrounding filler material will be less dense and not emissive. (The passive image may contain some contributions from the filler material due to scattering.) For ease of comparison, we normalize both images to a set average pixel value, and re-bin the active image to match the number of pixels and corresponding spatial size of the passive image. (In general, active radiography systems are expected to have much higher resolution). The algorithm then groups each pixel from the active image with the corresponding pixel from the passive image, and records the pair of intensities in a scatter plot. Figure 3 depicts this process. The deviation of the scatter plot data from the diagonal indicates whether the object contains distributed, emissive material. If the dense items in the active image line up with the bright items in the passive image, the method should yield a strong correlation. If, however, the image contains less distributed materials or significant dense, non-emissive material (such as a point source along with a lead brick), the active and passive images will not match, and the correlation between image data will be much weaker.

Repeating the above description in mathematical terms, the algorithm transforms each active pixel value  $A_{ij}$  and passive pixel value  $P_{ij}$  so that the average

of all the pixels in each transformed image is  $1/2$ . The value of  $x$  increases with higher density, whereas the value of  $y$  increases with higher emissivity.

$$x = -\frac{A_{ij} - \bar{A}}{A_{\max} - A_{\min}} + \frac{1}{2}, \quad y = \frac{P_{ij} - \bar{P}}{P_{\max} - P_{\min}} + \frac{1}{2}$$

The algorithm then computes the slope of the linear regression model of  $y$  as a function of  $x$ . Again, if the images were identical in the sense of having a positive linear relationship between pixel values, this value would be 1, whereas values far from 1 suggest little similarity between the active and passive images. Other metrics could be used to evaluate the similarity, such as the average deviation of each scatter plot point from the diagonal.

The key advantage of the pixel correlation algorithm is the lack of stored parameters for image analysis. Without stored sensitive comparison images or image parameters, the comparison can be carried out behind an information barrier. Eliminating stored sensitive parameters eliminates a fatal objection. While initial results are promising, as presented later in this paper, further evaluation is necessary to consider a number of practical limitations: the strong attenuation of the x-ray flux in conventional radiography, the perhaps sparse gamma-ray flux available for autoradiography, and the possible presence of other high- $Z$  materials, such as lead shielding in the case of stored plutonium oxide. One potential alternative is to have the inspection process use neutron flux to generate the active and/or passive images [10, 11], while another could be to consider isolated pixel regions with intensity above or below a threshold, rather than using every pixel in the image, some of which could contain incidental additional shielding.

## 5. Evaluation Data

We evaluated the performance of the three image analysis algorithms against a variety of real and simulated objects with different shapes, orientations, densities, and radioactive content, intended to test the relevant features of each algorithm. One set of objects consisted of six Marinelli beakers filled with epoxy having three different densities. Three out of these six beakers also included radioactive constituents homogeneously mixed in the epoxy. The total volume and densities were selected based on the parameters of the available radiography systems in the laboratory. Figure 4 gives the specifications of these objects. Orienting the Marinelli beakers in different directions produces radiographs such as those shown in Figure 5.

The beakers not containing radioisotopes were imaged with a Varian PaxScan 2520 radiography system in various orientations. We used these images of beakers without sources in evaluating the histogram comparison and pixel correlation algorithms.

Simulated images of the beakers containing radioactive isotopes were generated using MCNP [15] for a hypothetical passive imaging system. The model was based on the actual nuclides contained in the beaker as a source. The simulated passive imager consisted of an ideal pinhole camera with the aperture

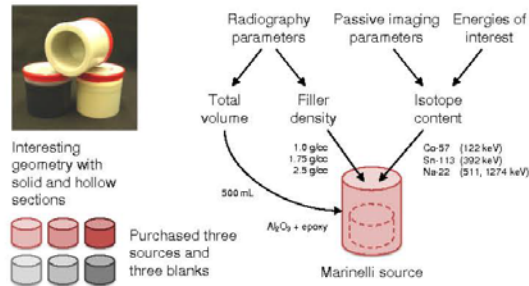


Figure 4: Marinelli beaker standards used for radiography.

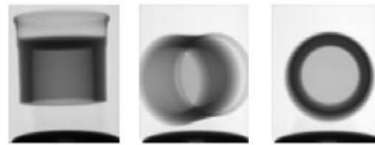


Figure 5: Example radiographs of Marinelli beaker standards in different orientations.

100 cm from the front face of the beaker. The pinhole had a diameter of 0.5 cm and was 9.8 cm from the image plane. The image plane itself was  $2 \times 2$  cm, containing  $150 \times 150$  pixels. Examples of the simulated passive images are shown in Figure 6. The resulting simulated active and passive images of the beakers were used for the pixel correlation algorithm.

In addition to the beaker objects, designed to test objects with complex shape, a second set of spherical objects was scanned with the active system to aid algorithm development, including rubber, quartz, and marble spheres. A bremsstrahlung source with beam endpoint energies of 110 keV and 160 keV was used to image several sizes of these spheres. Examples are shown in Figure 7.

Finally, we created a set of simulated objects for a hypothetical active imager based on the PaxScan, to test the material recognition algorithm described by this work. This dataset contained homogeneous spheres of diameter 3 cm to 13 cm, each consisting of either nominal wood, aluminum, iron, or lead. These simulated radiographs used a monoenergetic 800 keV or 1200 keV point source and a radiography tally in MCNP. The point source was placed 90 cm from the rear of the beaker and had an energy of 450 keV. The image plane was located 23 cm from the front face of the beaker. The dimensions of the plane were  $30 \times 30$  cm<sup>2</sup> with  $150 \times 150$  pixels. Figure 8 shows examples of the simulated sphere images. We used both the actual and simulated sets of sphere images

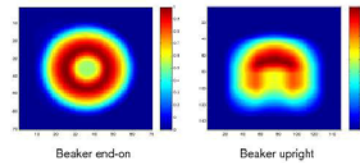


Figure 6: Example simulated passive images. Views of a Marinelli beaker containing a radioactive source with end-on (left) and upright orientation (right).



Figure 7: Example active images of spherical objects. Images of a rubber ball (left), quartz ball (middle), and marble (right).

to evaluate the material recognition algorithm, and values for the attenuation cofactors of the simulated materials were obtained by using MCNP to simulate the attenuation through unit thicknesses of each material.

## 6. Results

### 6.1. Histogram Comparison

We tested the histogram comparison algorithm on a set of fifteen active images of Marinelli beakers: five images in three groups according to density of epoxy. The images in each group were taken under identical conditions, with a slight shift in spatial position of the beaker between images. Figure 9 depicts the fifteen images and corresponding histograms. These histograms were constructed by binning the pixel intensities into 5,000 equal bins. One can

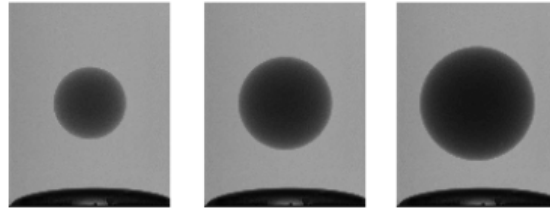


Figure 8: Example simulated active images of iron spheres.

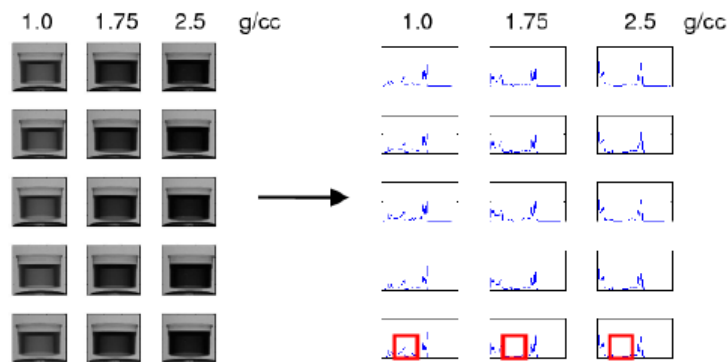


Figure 9: Marinelli beaker images and corresponding image histograms for evaluating the histogram comparison algorithm. The boxes indicate a particular feature difference across object densities.

observe particular feature differences between the histograms in each group, as indicated by the boxes in the figure.

Figure 10 shows the sample distributions of histogram comparison values for the within-group and across-group comparisons. The vertical axis shows the histogram comparison values generated by the histogram dot product, in arbitrary units. A strong separation is indicated, and is supported by the results of the two-sample  $t$ -test described in Section 4.1. The difference between within-group and across-group comparison values is highly statistically significant in all cases ( $p < 10^{-16}$ ).

Additionally, the histogram comparison showed no similarity between random groupings of the same images, as expected. In more realistic scenarios, the level of variation in images of objects of interest is likely to be much greater than that represented in the replicate measurements here, and further analysis on a broader range of image groups would be necessary to determine the full power of the approach. The results here show that the histogram comparison approach is very capable of distinguishing between the test objects of different

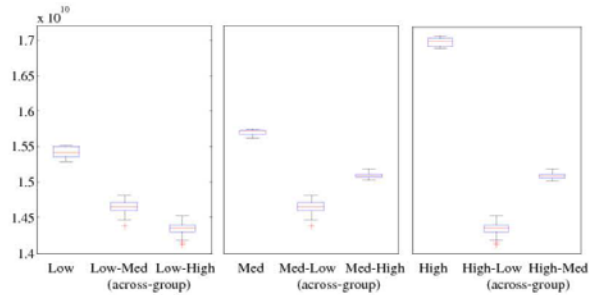


Figure 10: Box plot of within-group versus across-group histogram comparison values for the low-density Marinelli beaker images. Units are arbitrary. The boxes and “whiskers” indicate the extent of the values in each comparison group; inner bar: median; box: top and bottom quartiles; black bars: non-outlying extrema; external crosses: outliers). The across-group values are well separated from the within-group values.

densities and encourages such further study.

### 6.2. Material Recognition

We applied the material recognition algorithm to active images of real objects (including rubber, quartz, and marble spheres of several sizes) as well as simulated images of a range of materials, the details of which are described in Section 5. Figure 11 summarizes the results. Each point in the figure corresponds to a sphere of different radius and material.

The approach results in good discrimination between materials for both real and simulated images. The estimated  $\mu$  for the large and small rubber spheres was very similar, while the estimated  $\mu$  varied greatly between the rubber and marble spheres, even when these objects were similar in size. Even the densest objects considered in simulated images produced well-separated  $\mu$  estimates for all seven sizes of spheres considered (noting the higher beam energy used for the simulations). Moreover, the estimates of this effective attenuation factor are very close to “true” values of the attenuation factors used for image simulation. This result supports further study of the material recognition algorithm for use in verification based on material identification as well as discrimination.

In some cases, only portions of sphere images are available for analysis. For example, additional objects may occlude parts of the sphere being examined. Alternatively, the effective transmitted flux may drop to zero in regions where the object is too thick or dense. We studied the effect of both these scenarios on

## 6.3 Active/Passive Pixel Correlation

15

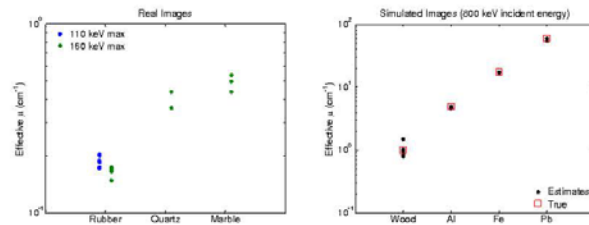


Figure 11: Results of the material recognition algorithm on real and simulated images of spheres. Each plotted point corresponds to a sphere of a different radius and material.

the resulting  $\mu$  estimates for the simulated spheres. As a baseline for determining minimal requirements, our image-extracted  $\mu$  estimates were required to be within 10% of the calculated true value, and within 5% precision based on confidence intervals produced by the “sphere fitting” nonlinear regression described in Section 4.2.

Figure 12 depicts the minimum portions of the simulated images necessary for the material recognition algorithm to produce estimates that meet the criteria above. The incident energy was 1200 keV in this case. Using only the outer ring (annulus) of each sphere image to estimate  $\mu$  (simulating the effect of total beam absorption inside that outer ring), the accuracy and precision requirements were met for the denser objects (Al, Fe, Pb, and W) when the annulus consisted of only 36% of the full area for all sphere sizes, the annulus thickness being approximately 20% of the distance from the outer edge to the center of the sphere image. A lower percentage was needed for the larger spheres. We also studied the effects of occlusion by blocking out all pixels above a line through the sphere image. Again, the algorithm had good performance for denser objects at all sizes when only 7.2% of the full image could be used, using pixels from the outer edge to approximately 25% of the distance from the outer edge to the center.

## 6.3.3 Active/Passive Pixel Correlation

To evaluate the pixel correlation algorithm, we took a real active image of the low-density Marinelli beaker in an “end-on” configuration. This image appears in Figure 5 at the far right. We then simulated passive images on the same beaker in the “end-on” configuration, tilted 70 degrees, and upright. Furthermore, we created simulated images of a random configuration (pixels uniformly distributed between 0 and 1) and a point source. Figure 13 illustrates the output of the pixel correlation algorithm. The plot on the left contains the noisy data from the images, whereas the plot on the right depicts the linear regression lines for the scaled data. The correlation values for these images are reported in Table 1. As expected, a near-perfect correlation is obtained from the active-passive

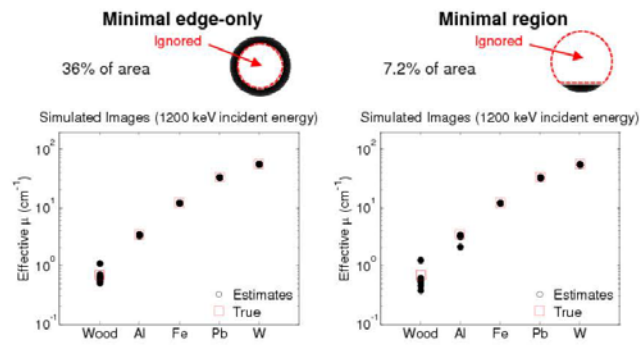


Figure 12: Results of the material recognition algorithm on reduced portions of simulated sphere images. Each plotted point corresponds to a sphere of a different radius and material. Schematics above indicate minimum portions necessary for relatively accurate and precise estimates. Left panel corresponds to a minimal number of pixels in an outer annulus; right panel corresponds to minimal number of pixels in from the edge to a line across the image.

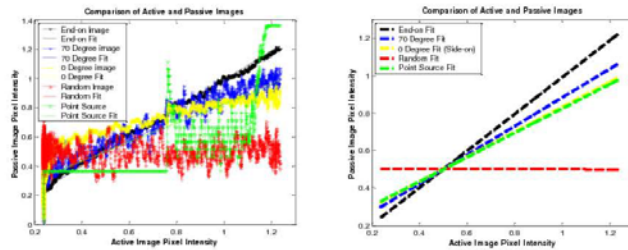


Figure 13: Results of pixel correlation algorithm. An active image of the Marinelli beaker in “end-on” configuration was compared to various simulated passive images. The plot on the left shows the individual correlation values, whereas the plot on the right gives the linear regression lines.

Table 1: Correlation values for pixel correlation algorithm, relative to “end-on” active image of Marinelli beaker.

Passive image	Correlation
Beaker end-on	0.98
Beaker tilted 70 degrees	0.77
Beaker upright	0.67
Random field	0.01
Point source	0.65

comparison of end-on images, while a steadily decreasing correlation is found as the passive image varies, ultimately yielding no correlation for a random image.

The results quantitatively demonstrate the concept of pixel correlation and suggest that this approach may be useful as a verification concept.

## 7. Discussion and Conclusions

We have presented a basis for three possible techniques for analyzing imaging information in a possible Arms Control context. These algorithms are designed to avoid the tradeoffs between unambiguous object verification and applicability to environments where full images may not be retained. Each technique has well-posed and clear-cut technical implementation challenges to be addressed from an information security standpoint. Specifically, the fundamental question that arises with the histogram comparison algorithm is whether a balance between non-invertibility and verification can be struck, and we believe that this question can be rigorously addressed using mathematical analysis. The material recognition algorithm might be well suited to a chemical form attribute that enables discrimination between such materials, but may be significantly more challenging for more complex geometries and in the presence of greater image clutter. The pixel correlation algorithm rigorously satisfies IB constraints

since it does not rely on any stored information at all, but may need to use a more complex analysis to recognize distributed SNM in the presence of other shielding. Together with knowledge of the radiography systems, the use of these techniques, alone or in combination, can potentially improve verification capability and increase the likelihood of detecting material diversion.

The algorithms can be improved in several ways. For subtly differing images with a high degree of internal complexity, histogram comparisons seem to perform well, providing sensitive image discrimination without resorting to the addition of noise or averaging of pixels to achieve information security. However, this may not be the case when imaged objects are simpler, or detector settings fluctuate or are unknown. Therefore, further study must consider these metrics against such images, and should develop other metrics to examine differences between simpler objects. The material recognition algorithm as it was tested presupposed the location of a circular object within the image and an accurate measurement of its location and radius. Additional noise is expected when this method is applied to images with objects of unknown size and location, and further work should provide a complete analysis of the resulting uncertainties. The pixel correlation technique has been performed on a variety of images, but its actual performance will depend strongly on the variety and sensitivity of the passive gamma ray imaging system used. A real passive system for inspection will need to employ an imaging system having resolution at least similar to the expected number of spatial bins needed for the analysis methods outlined in this work. Furthermore, this technique presupposes minimal additional material or structure. Further research must determine its sensitivity when additional material is present.

#### Acknowledgment

We gratefully acknowledge the Laboratory Directed Research and Development program for funding this research at Pacific Northwest National Laboratory. Pacific Northwest National Laboratory is a multiprogram national laboratory operated by Battelle Memorial Institute for the US Department of Energy under Contract DE-AC05-76RL01830.

#### References

- [1] Technology R&D for Arms Control, Tech. Rep. NNSA/NN/ACNT-SP01, Office of Nonproliferation Research and Engineering (ONRE), U.S. Department of Energy (Spring 2001).
- [2] J. Fuller, Verification on the road to zero: Issues for nuclear warhead dismantlement, Arms Control Today.
- [3] R. T. Kouzes, J. L. Fuller, Authentication of monitoring systems for non-proliferation and arms control, in: Proc. Symposium on International Safeguards: Verification and Nuclear Material Security, International Atomic Energy Agency, Vienna, Austria, 2001, IAEA-SM-367/17/05.

- [4] R. Whiteson, D. W. MacArthur, Information barriers in the trilateral initiative: Conceptual description, Tech. Rep. LAUR-98-2137, Los Alamos National Laboratory, Los Alamos, New Mexico (1998).
- [5] M. R. Smith, J. Dunn, K. Seager, Future directions for arms control verification technologies, in: Proc. INMM 2010 Annual Meeting.
- [6] E. E. Fenimore, T. M. Cannon, Coded aperture imaging with uniformly redundant arrays, *Applied Optics* 17 (3) (1978) 337–347.
- [7] J. F. Morgan, G. Ignatyev, D. Semenov, M. Chernov, Gamma-ray camera for arms control applications, in: Proc. SPIE, Vol. 3769, 1999, pp. 24–30.
- [8] A. Busboom, H. Elders-Boll, H. D. Schotten, Uniformly redundant arrays, *Experimental Astronomy* 8 (1998) 97–123.
- [9] M. J. Myjak, J. S. Rohrer, S. J. Morris, M. L. Woodring, J. H. Ely, Pulse processing system for the RADMAP radiation modulation aperture imager, in: Proc. 2007 IEEE Nuclear Science Symposium.
- [10] P. A. Hausladen, P. R. Bingham, J. S. Neal, J. A. Mullens, J. T. Mihalcz, Portable fast-neutron radiography with the nuclear materials identification system for fissile material transfers, *Nuclear Instruments and Methods in Physics Research Section B: Beam Interactions with Materials and Atoms* 261 (1–2) (2007) 387–390.
- [11] J. T. Mihalcz, J. K. Mattingly, J. S. Neal, J. A. Mullens, NMIS plus gamma spectroscopy for attributes of HEU, PU and HE detection, *Nuclear Instruments and Methods in Physics Research Section B: Beam Interactions with Materials and Atoms* 213 (2004) 378–384.
- [12] C. Nickel, X. Zhou, C. Busch, Template protection via piecewise hashing, in: *International Conference on Intelligent Information Hiding and Multimedia Signal Processing*, 2009, pp. 1056–1060. doi:<http://doi.ieeecomputersociety.org/10.1109/IIH-MSP.2009.234>.
- [13] P. J. Bickel, K. A. Doksum, *Mathematical Statistics*, Prentice Hall, Englewood Cliffs, New Jersey, 1977.
- [14] R. O. Duda, P. E. Hart, Use of the Hough transformation to detect lines and curves in pictures, *Communications of the ACM* 15 (1) (1972) 11–15.
- [15] The X-5 Monte Carlo Team, MCNP—a general n-particle transport code, version 5, Tech. Rep. LA-UR-03-1987, Los Alamos National Laboratory, Los Alamos, New Mexico (1987).



**Pacific Northwest**  
NATIONAL LABORATORY

*Proudly Operated by **Battelle** Since 1965*

902 Battelle Boulevard  
P.O. Box 999  
Richland, WA 99352  
1-888-375-PNNL (7665)

[www.pnl.gov](http://www.pnl.gov)



U.S. DEPARTMENT OF  
**ENERGY**